Design, Fabrication And Application Of A Dedicated Thick-film Hybrid Time Domain Reflectometer

by

Joel Edwin Keys Jr.

Thesis submitted to the Faculty of

Virginia Polytechnic Institute and State University

in partial fulfillment of the requirements for the degree of

Master of Science

in

Electrical Engineering

APPROVED:

Dr. Sedki M. Riad, Chairman

Dr. Aicha Elshabini-Riad

Dr. F. William Stephenson

April 13, 1987

Blacksburg, Virginia

Design, Fabrication and Application of a Dedicated Hybrid Thick-film Time Domain Reflectometer

by

Joel Edwin Keys Jr.

Sedki M. Riad, Chairman

Electrical Engineering

(ABSTRACT)

This work presents a design process for developing a dedicated hybrid thick-film time domain reflectometer. The design process allows for variation of the pulse generator characteristics as well as the output impedance of the unit. The unit is fabricated using standard thick-film hybrid techniques while giving consideration to problems encountered at microwave frequencies. This thesis also presents an overview of time domain reflectometry and its applications. Special emphasis is given to the problem of characterizing material dielectric constants using delay measurements.

Acknowledgements

The author wishes to thank Dr. Sedki M. Riad for his support, guidance and patience throughout this work.

Special thanks are also extended to Dr. Aicha Elshabini-Riad and Dr. F. W. Stephenson for their aid and direction.

Sincere thanks are given to for his invaluable assistance and good humor.

Credit and support is also given to , longtime friend, coworker and roommate for his help, patience and advice.

The author also wishes to thank his parents for their support, both moral and economic, during his studies. Without them, none of this would have been possible.

Additional thanks are extended to my brother, , my sisters and for their "long-distance" encouragement.

Special credit should also be given to the students and staff members of the

Time Domain and Hybrid Microelectronics Laboratories for their assistance in times of crisis.

The Soilmoisture Equipment Corporation is also recognized for their supposrt of research in this area.

Table of Contents

Chapter 1

INTRODUCTION

This work presents a design process and design evolution of a time domain reflectometer. The design was developed for a dedicated soil moisture meter application but can also be modified or extended to other specific TDR applications.

Time domain reflectometry (TDR) is a microwave measurement technique used to determine the electrical characteristics of a network, circuit or device. It is similar in concept to a radar or sonar system where a pulse is sent out and the reflections are analyzed. TDR is capable of finding the responses of a system over a bandwidth which extends from DC to the GHz range. The bandwidth is governed by the properties of the generated pulse. In general, the faster the transition duration of the pulse, the wider the bandwidth of the TDR unit. TDR can be used to measure the electrical properties of materials which can then be related to the physical properties. The application of measuring the moisture content of soils relies on this capability.

The design specifications for this TDR were to produce a 0.6 volt 50Ω matched-load pulse with a 200 ps transition duration. The baseline and topline ripple should be of the order of 5%. An equivalent time sampling gate capable of observing such a pulse was also required along with all the associated electronics necessary for proper operation. The sampling window was required to be of sufficient duration to allow direct observation of at least 100 meters of cable. The TDR unit also had to be battery powered for portability. This limited the available power supply voltages to ± 15 volts.

The thesis is organized into six chapters, the first of which is this introduction. Chapter 2 discusses the technique of time domain reflectometry in detail. It also compares TDR to frequency domain measurement techniques and highlights the advantages of both techniques. Chapter 3 details the individual subsystems that make a TDR unit. Specific attention is focused on the requirements of this dedicated TDR and the steps involved in meeting these requirements. Chapter 4 details the advantages, materials and processing requirements of thick-film hybrid microelectronic fabrication. This chapter also discusses the problems and solutions associated with hybrid designs at microwave frequencies. Chapter 5 details the testing and tuning steps necessary for proper TDR function after fabrication using hybrid techniques. Emphasis is placed on the problems associated in the design requiring a minimum number of components. Finally, Chapter 6 summarizes the thesis, the design process, TDR techniques and presents suggestions for future work in TDR fabrication and application.

Chapter 2

Time Domain Reflectometry

2.0 Introduction

Time domain reflectometry (TDR) is a technique used to find the transient responses of a system, device or structure. It can simply be described as a technique whereby a voltage pulse (step or impulse) is transmitted into the device or structure to be tested. The reflections of the device or structure can then be analyzed to determine certain properties of the tested device or structure. The bandwidth of the technique is governed by the transition duration of the step or impulse itself. In simple terms, the faster the transition, the higher the upper cutoff frequency.

A discussion of frequency domain measurement techniques will be also be reviewed. Some comparisons between TDR and direct frequency measurement will be presented with emphasis on their inherent ability to extract the necessary information for the soil moisture TDR unit.

2.1 Typical TDR Applications

As indicated above, TDR is used to gain information about a device or material. The most common usage of TDR is to measure the impedance of transmission lines and to identify the location of any discontinuities along the line. Other information such as loss in the transmission line and the effective dielectric in a particular region can also be obtained [1].

2.1.1 Impedance measurements

For the general network shown in Figure 2.1.1.1 (a), the voltage reflection coefficient due to a resistive mismatch is given by Eq. (2.1).

$$\rho_L = \frac{E_r}{E_i} = \frac{R_L - R_0}{R_L + R_0} \qquad (2.1)$$

For the cases where $R_L = R_0$, 0 or infinity, $\rho = 0, -1$ or $+1$ respectively. The velocity of propagation, ν, depends on the dielectric constant, ϵ_r, of the material in R_L and is given by $\nu = c/\sqrt{\epsilon_r}$ for simple media, where c is the speed of light in a vacuum. TDR can be used to find the impedance of any load provided the impedance differences are large enough and are separated by a sufficient distance. As a general rule, if two discontinuities are located closer together than one-fourth the transition duration of the pulse, they may be identified as one single discontinuity [1].

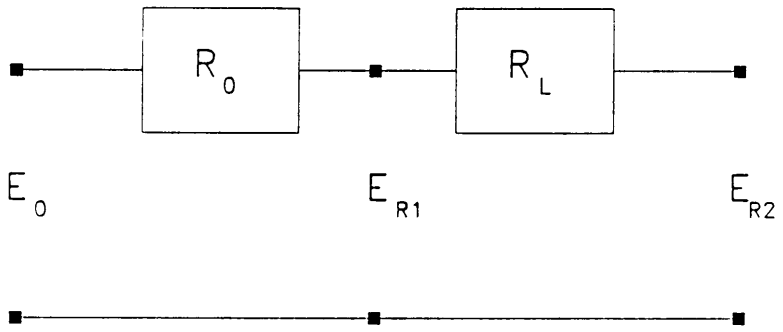

Figure 2.1.1 (a) A general network.

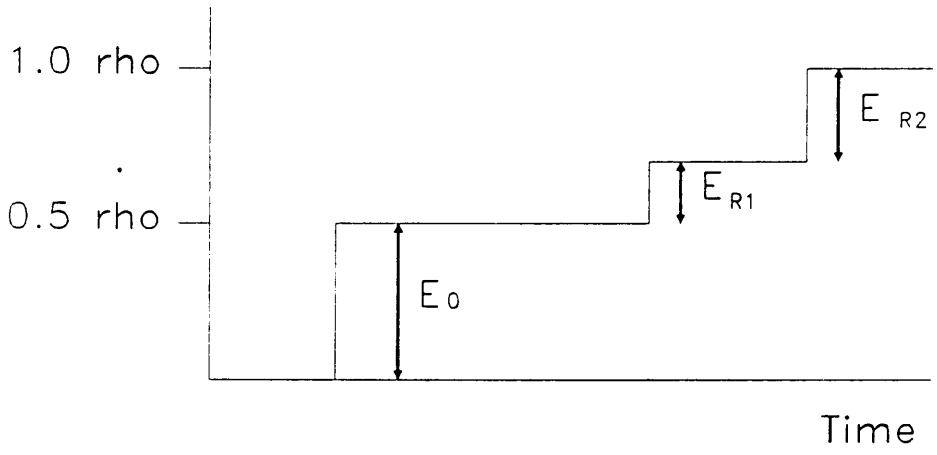

Figure 2.1.1 (b) TDR trace for an unknown impedance cable.

In the common application of transmission line or cable testing, TDR traces are easily interpreted to determine the impedance of the unknown line. For example, the TDR trace of an unknown cable connected to a 50Ω TDR unit is shown in Figure 2.1.1.1 (b). Equation 2.1 can be solved in terms of R_L to yield the relationship:

$$R_L = R_0 \frac{1 + \rho}{1 - \rho} \qquad (2.2)$$

For this example, $\rho = 0.2$, and the impedance value of the unknown cable is found to be 75Ω. The length of the cable can also be determined from the TDR trace by observing the time from the beginning of the 75Ω section to the open circuit seen later. The velocity of propagation in the cable must be given, so the distance is then related to the observed time by:

$$\text{length} = \frac{t * c}{2\sqrt{\epsilon_r}} \qquad (2\text{-}3)$$

2.1.2 Reactive component measurement

The preceding section assumed that a pure resistance was the only electrical property being measured. In general, TDR can be extended to measure and categorize reactive discontinuities as well. For example, in the case of a series resistance and capacitance shown in Figure 2.1.2.1 (a), the TDR response can be used to estimate both component values. Figure 2.1.2.1 (b) shows the waveform generated by such a network. Other networks can be measured in the same way by first solving the response of the network to a unit step function through LaPlace or

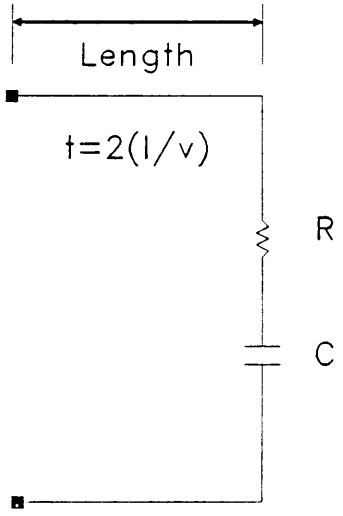

Figure 2.1.2.1 (a) A series RC network.

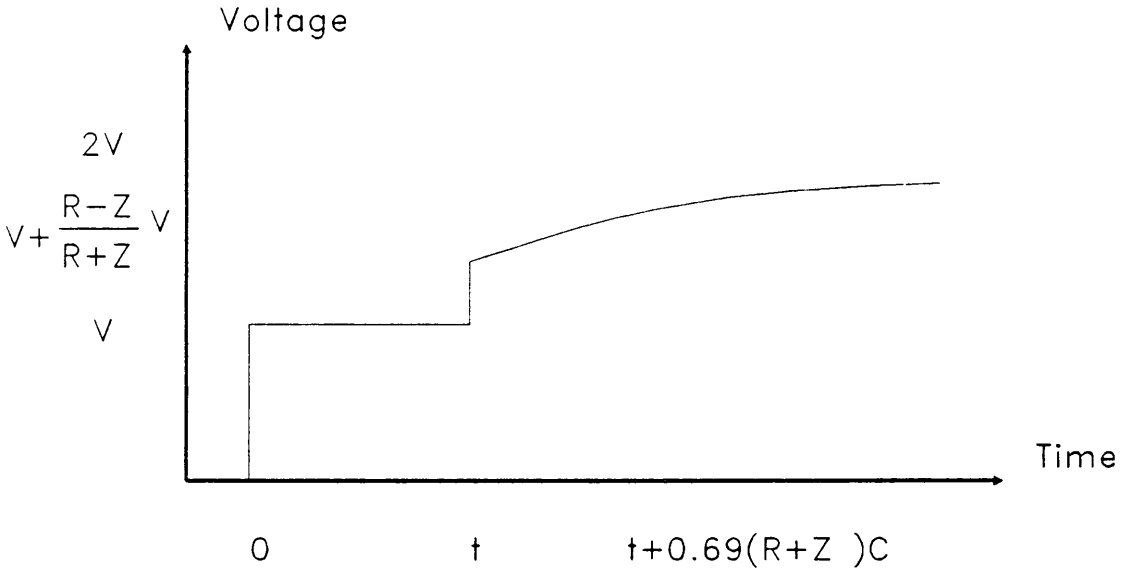

Figure 2.1.2.1 (b) TDR trace for the RC network.

Fourier transform techniques [2]. If multiple discontinuities are observed, a model of the system can be created using discrete elements separated by lengths of delay lines.

2.1.3 Loss measurements

TDR also provides a simple means of observing and characterizing losses in transmission line structures. If there is a series loss due to low conductivity in the conductor, or skin effect, an exponentially rising response will be observed. In the case of shunt losses, due to a poor dielectric in a coaxial line for example, there would be an exponential decay. This is intuitively obvious as the line would have a progressively lower impedance as the pulse propagates down it. As mentioned above, these loss mechanisms can be modelled and the magnitude of their effects measured using TDR.

2.1.4 TDR system effects

The pulse generator has two characteristics which will affect the measurements it is capable of performing. The first is the internal impedance of the TDR unit. The microwave standard for measurements is 50Ω and most TDR units are fabricated with this impedance value. If the system to be tested has a different impedance, 75Ω for example is a standard impedance in video equipment, distortions of the TDR display may result from this mismatch. Multiple reflections between regions of varying impedance can be seen at later times in the TDR display. To determine the number of such problems, a matched load can be placed in the TDR line and these effects can be seen prior to attaching the test structure. This ability to locate

discontinuities is a useful property of TDR. A common application of this property may be found in the telephone industry. A TDR unit may be connected to a telephone line and the distance to a break (open circuit) can be quickly found.

A second problem has to do with the bandwidth of the TDR system. As mentioned previously, the transition duration governs the upper cutoff frequency [3]. It can be shown that the relationship is empirically given by

$$BW \approx \frac{350}{\text{Transition Duration (ps)}} \text{ [GHz]} \qquad (2\text{-}4)$$

The 200 ps risetime specification for the TDR soil moisture corresponds to a bandwidth of approximately 1.75 GHz.

2.2 Delay measurements

The preceding sections covered general uses of time domain reflectometry for microwave measurements. The soil moisture meter which will employ TDR techniques relies on obtaining the dielectric constant, ϵ_r, of the soil. This value can be related to the moisture content of the soil. The probe used is a pair of parallel steel rods which form a transmission line. As can be seen from Eq. 2-3, the length of the transmission line is related to the velocity of propagation in the line and the time measured. If the length is known, and the time obtained from the TDR waveform, the effective dielectric constant can be calculated.

For regions for which $\epsilon_r > 1$, the velocity of propagation would be reduced

compared to a vacuum and the apparent, or electrical length, of the line would increase. If multiple layers of dielectric with significantly different ϵ_r are placed in the transmission line, the reflection coefficient from layer to layer will also be affected in addition to the delay effect. Figure 2.2.1 (a) gives the response of the probe in air and (b) shows the response when a dielectric medium is placed between the conductors.

There are some problems associated with this technique to measure dielectric constants. If the dielectric is lossy, the signal may be so attenuated as it travels down the line that the reflection may never be seen. It may be possible to increase the amplitude of the pulse generator to overcome these effects, and this was one of the reasons behind the amplitude specification of the developed TDR unit. If the value of ϵ_r is not a constant throughout the region, some form of average value is obtained. It may be possible to characterize the gradient of ϵ_r along the probe line and relate that to various material characteristics. Another problem can arise in determining where in the TDR waveform a transition actually occurs. Dispersion and loss will slow down the transition which can make its exact determination difficult.

In addition to these possible problems, the probe itself can create distortions of the TDR waveform. The probe being used in the soil moisture application has several characteristics which affect the accuracy with which the delay measurement can be performed. The steel transmission line rods are spaced by a distance which yields a characteristic impedance of 200 Ω. Since the TDR has a designed source impedance of 50 Ω, a wideband 4:1 transformer is used to match the probe and the TDR unit. This transformer, called a balun, is limited in bandwidth to 1.5 GHz.

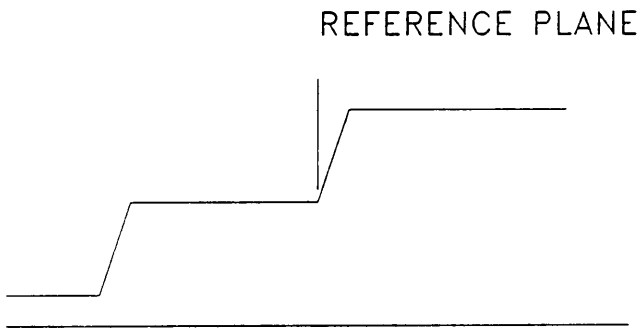

Figure 2.2.1 (a) TDR trace for a probe in dry soil.

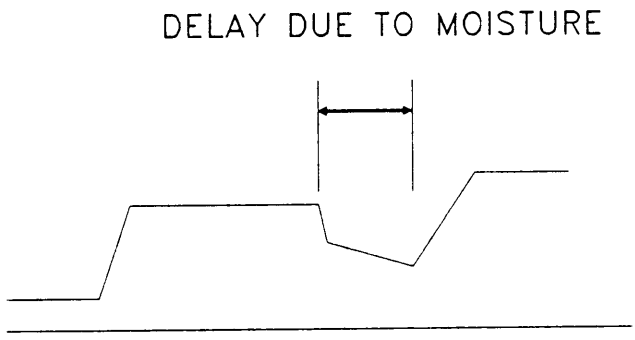

Figure 2.2.1 (b) TDR trace for a probe in moist soil.

The balun distorts the waveform due to the large inductive and capacitive loading of this element. It can distort the sampling system used to observe the TDR waveform. Modelling of the probe may be accomplished to isolate and categorize these effects. Once the problems are identified, it may be possible to improve the probe or change the TDR system to compensate for these effects.

2.3 Frequency domain measurements

Using the wideband step voltage to stimulate a test structure in TDR yields the frequency response for that structure over the entire bandwidth simultaneously. It is possible to perform a Fourier transform of the TDR response to determine the structure response at any given frequency [4,5]. This assumes, however, that the network under test is linear, otherwise harmonic mixing can occur and distort the TDR response [3]. An alternative, well developed, test method entails direct frequency measurements. A sinusoidal oscillator can be used to stimulate the test structure and the response of the system at that frequency can be obtained. By sweeping the oscillator through a range of frequencies, the wideband response can be measured.

There are a number of difficulties associated with such a technique. The source itself can be difficult and expensive to fabricate. Maintaining a harmonic-free sinusoid at microwave frequencies is a problem. The connections to the device being tested will also affect the response of the network. As a result, the hardware required to accurately perform frequency domain measurements is several times more expensive than a similar bandwidth TDR system [3].

2.4 S-parameter measurement techniques

A device or structure can be represented as a black box with multiple ports leading into and out of the box as illustrated in Figure 2.4.1 (a). If a wave is transmitted into one port, parts of the wave can be transmitted to any other port and some of the wave can be reflected back to the port through which it entered. A matrix equation relating the response at any port to the stimulation at any port and the network effects can be generated as shown in Figure 2.4.1 (b). The network response parameters are called scattering or S-parameters as they are determined by the way the incident waves are scattered through and by the network [6]. Measuring individual S-parameters can be difficult so a simple example of a 2-port network is presented. However, the concept can be extended to a n-port network.

The equations for a generic 2-port network are given in Equation 2-6. The incoming signals are designated as "a" and the responses are designated by "b". The four S-parameters for such a system are indicated. Writing the governing equations for the responses results in two simple relationships

$$b_1 = s_{11}a_1 + s_{12}a_2$$

$$b_2 = s_{21}a_1 + s_{22}a_2 \qquad (2\text{-}6)$$

The process required to determine the individual S-parameters is quite straightforward. If, for example, s_{11} is to be evaluated, the ratio of b_1/a_1 will give the correct response provided a_2 is equal to zero. Similar defining equations can be derived for each S-parameter.

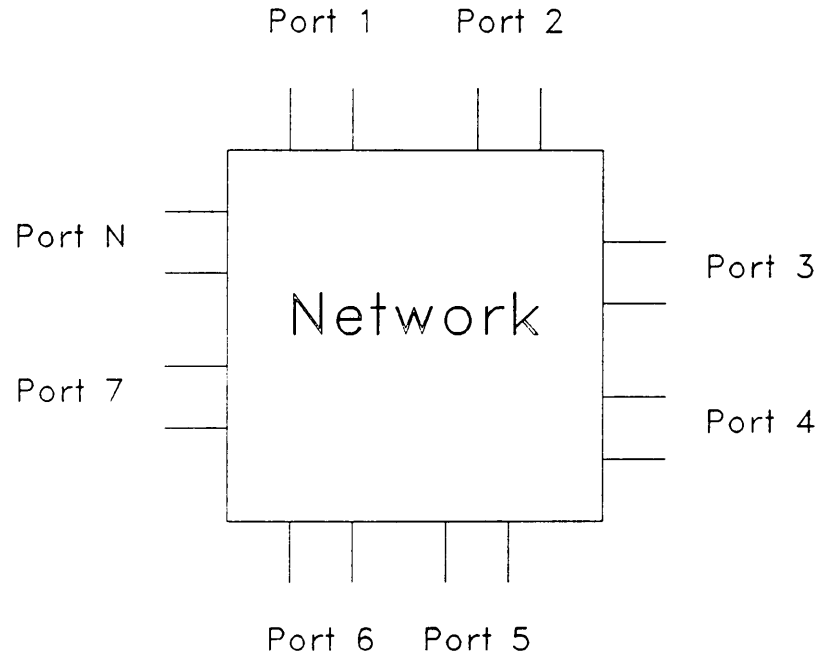

Figure 2.4.1 (a) A N-port microwave network.

$$\begin{bmatrix} b_1 \\ b_2 \\ b_3 \\ \\ b_N \end{bmatrix} = \begin{bmatrix} s_{11} & s_{12} & s_{13} & & s_{1N} \\ s_{21} & s_{22} & & & \\ s_{31} & & & & \\ & & & & \\ s_{N1} & & & & s_{NN} \end{bmatrix} \begin{bmatrix} a_1 \\ a_2 \\ a_3 \\ \\ a_N \end{bmatrix}$$

Figure 2.4.1 (b) The matrix equation of S-parameters for an N-port network.

From a practical measurement standpoint, obtaining the actual S-parameters can be difficult. In the case of a frequency domain measurement approach, some form of directional coupler is required to allow the source to stimulate the network while preventing the source from directly affecting the measurement system. Time domain has a simpler connection as the source appears at a different time than the response in the TDR waveform and can be easily ignored. For the above example of finding s_{11}, either approach requires that the port at node 2 be impedance matched to eliminate the source at that node. This match and the various connections can be difficult to accurately achieve.

2.5 Conclusions

Both frequency domain and time domain techniques may be used to obtain information about a system at microwave frequencies. Frequency domain techniques had been developed because of the reduced data processing this approach requires. Furthermore, early TDR systems had lower signal to noise ratios than equivalent frequency domain systems. Advances in components and computer technology have narrowed this gap.

The soil moisture meter application requires a simple and fast technique to obtain the effective dielectric constant of a sample which can then be related to the moisture content. This type of measurement is best performed using TDR since the basis for the test is one of measuring a delay. The cost and complexity of the TDR hardware is also much simpler than that for a equivalent frequency domain meter.

Chapter 3

TDR System Requirements

3.0 Introduction

This chapter will discuss what electronics are necessary to realize a time domain reflectometer. It will focus on the various subsystems required and the variety of ways by which they can be designed and adapted to a specific task.

Typical TDR units consist of three basic subsystems: a pulse generator, a sampling network and an output/feedback circuit. In addition, several timing and control signals are necessary to link the action of each subsystem for proper function. Figure 3.0.1 shows the block diagram of all the basic parts of a TDR [7]. Each of these subsystems was designed separately and then integrated to form the complete TDR unit.

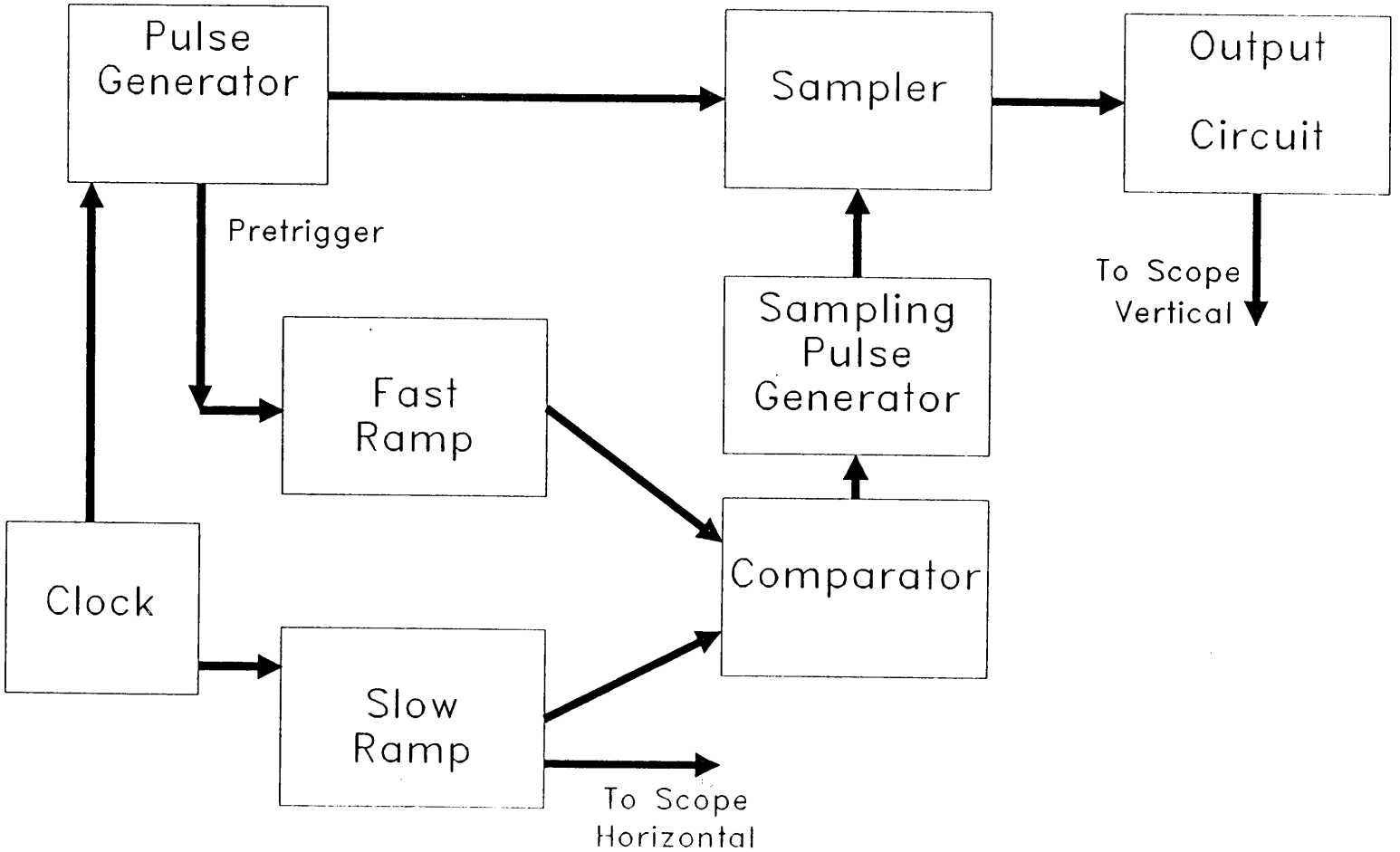

Figure 3.0.1 The basic components of a TDR unit [7].

3.1 Pulse generator circuits

The pulse generator is the heart of the TDR unit. It provides the wideband signal necessary in either impedance or delay measurements as described above. There are a variety of electronic devices which can be used to generate the fast transition pulses required in TDR systems. These include tunnel diodes, step recovery diodes and avalanche transistors. Each of these devices and their associated advantages and disadvantages will be characterized.

The requirements of the pulse generator for the soil moisture meter application were to have an amplitude of 0.6 volts into a 50Ω load and have a transition duration of ≤ 200 psec. This would yield a bandwidth of about 1.75 GHz. Later requirements were for a very clean waveform with ≤ 5% baseline ripple and ≤ 8% topline ripple. Figure 3.1.1 defines these various waveform parameters.

3.1.1 Tunnel Diodes

The tunnel diode is a simple *p-n* junction in which the impurity doping concentrations are high enough to have forced both regions to be degenerate materials. This doping forces the Fermi level to be located within the allowable bands of both the conduction and valence bands. The high doping levels also force the depletion width to be of the order of 100 Å which is smaller than the depletion region width in regular *p-n* diodes [8].

The principle of tunneling requires that there be a narrow barrier region through which there is a finite probability that an electron can "jump" through to a

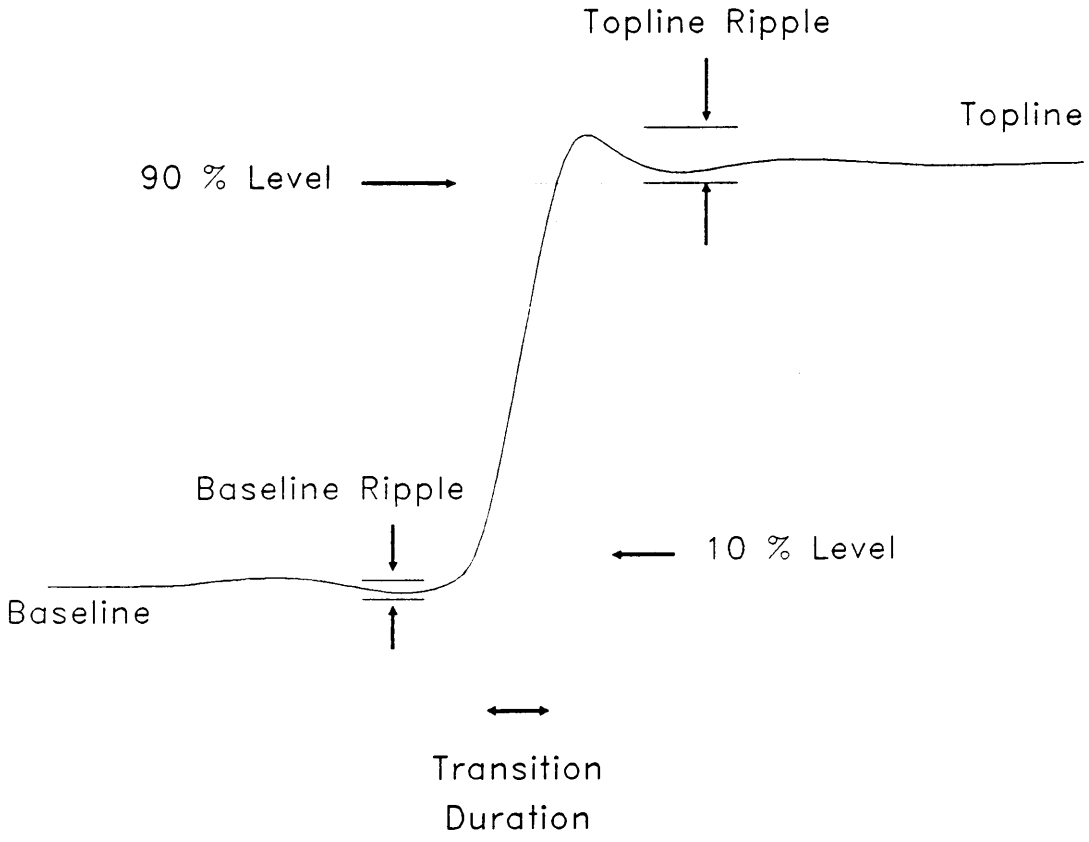

Figure 3.1.1 Basic waveform parameters and definitions.

vacant site on the other side of the barrier despite having less energy than the barrier itself. During operation, a forward voltage is applied which generates a tunneling current [9]. This current increases to a peak when the bottom of the valence band and the top of the conduction band coincide. At this point, the current begins to decrease with increasing voltage, giving rise to a differential negative resistance. Eventually, the tunnel diode current would again begin to increase exponentially due to thermal generation of carriers, as in a regular diode. The transition from the peak to the valley current occurs rapidly which gives rise to a wideband signal. Figure 3.1.1.1 shows the I-V relationship for a tunnel diode. To use a tunnel diode as a pulse generator, the diode is biased to just below the peak current value. A small voltage trigger is then applied to force the valence and conduction bands apart. The current through the diode rapidly decreases. Figure 3.1.1.2 shows a simple tunnel diode pulse generator. As the diode current decreases, the current through R_L increases giving rise to the desired pulse [10].

Germanium tunnel diodes can produce transition durations on the order of 30 ps. These generated pulses are step functions which are very clean i.e. ripple free, however, the amplitude is limited to about 0.25 volts into a 50Ω load. Several commercial TDR systems, Tektronix 1502 and Tektronix S-52, use tunnel diodes to produce wideband pulses. As these units are designed for use in laboratory measurements, the low amplitude does not cause problems.

3.1.2 Step Recovery Diodes (SRD)

The step recovery diode is a class of charge storage diodes which conduct in the reverse bias mode for a short period and then cut off abruptly. These diodes are

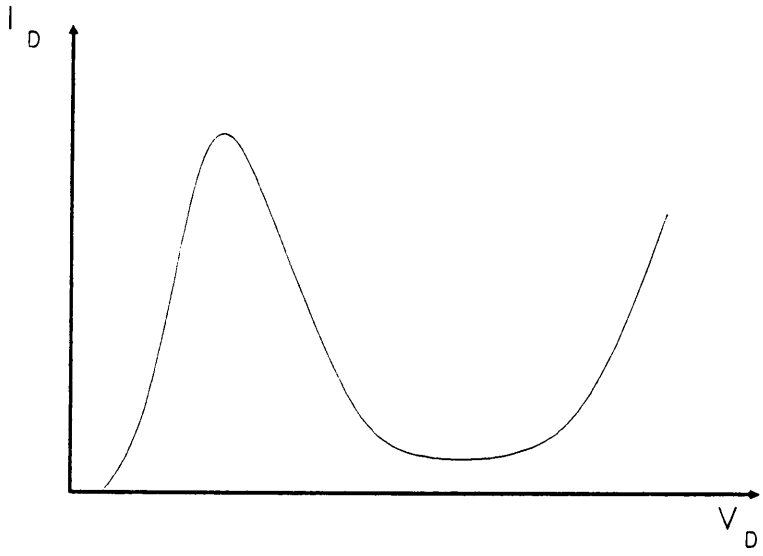

Figure 3.1.1.1 I-V curve for a tunnel diode [10].

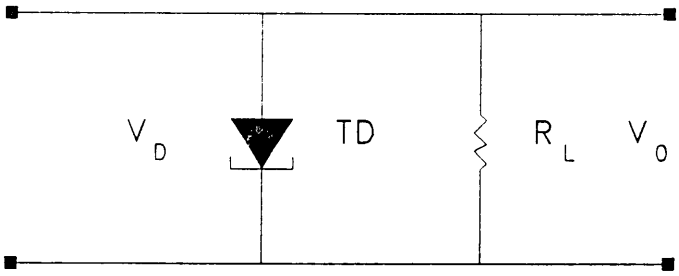

Figure 3.1.1.2 A tunnel diode pulse generator [10].

formed by placing an intrinsic layer of material between the *p* and *n* regions. The principle of operation requires that the SRD be forward biased to build up charge in the depletion region. The diode is then reverse biased by a step voltage. The diode will continue to conduct until all of the stored charges have been depleted. At this time, the diode rapidly switches to a non-conducting (high-impedance) mode. This cutoff occurs on the order of picoseconds and creates a fast transition pulse which is rich in harmonic content [8].

The SRD is not a pulse generator itself but is used to sharpen the transition of the reverse bias step. In this respect, the SRD is attractive as the amplitude of the step can be raised to several volts. Figure 3.1.2.1 shows a simple SRD pulse sharpening network. The capacitors are used to prevent the DC bias from affecting the rest of the network [11]. There are, however, a few inherent problems found when using step recovery diodes in pulse generator applications. When the reverse bias is initially applied and during the time charges are being depleted, the voltage does not remain at exactly the baseline of the step. Rather, it rises to about $0.1 \simeq 0.2$ volts. This prestep is visible until the diode completely depletes the stored charge. At that time, the SRD snaps off quickly. Another problem is the topline of the signal has a great deal of ringing. Figure 3.1.2.2 shows the response of an SRD to a step input. The step input transition duration is about 1 nsec and the SRD sharpens this to about 100 ps.

Additional electronics are necessary to clean the output waveform of the SRD. The first area to be addressed is the prestep. An effective solution is to add a Schottky diode in the signal line [12]. The diode is not forced into conduction by the prestep so the output remains at the baseline. The main, high speed, pulse is of

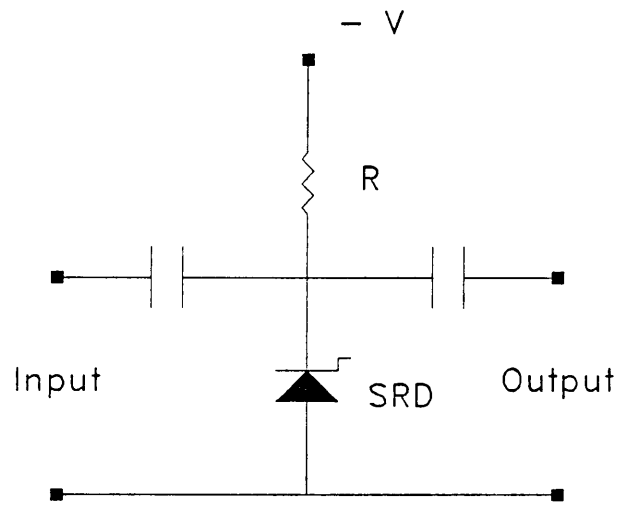

Figure 3.1.2.1 A basic step recovery diode pulse sharpening circuit [10].

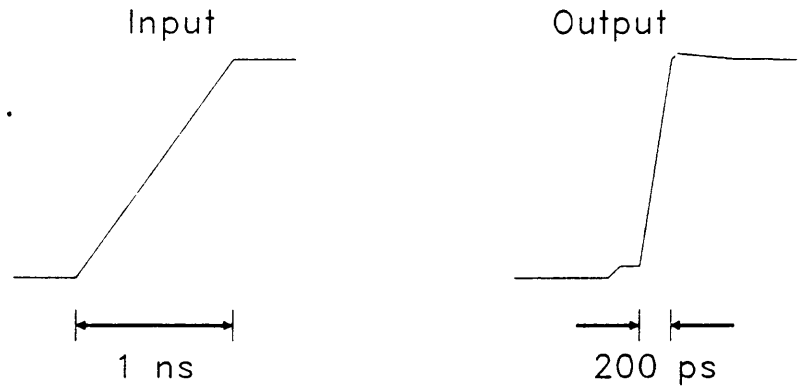

Figure 3.1.2.2 The input and output signals of the SRD sharpening circuit.

sufficient voltage to force the Schottky diode into conduction, resulting in a clean baseline voltage. This waveform improvement typically results in a slower transition speed.

The ringing on the topline of the pulse is due to high-order harmonics generated by the SRD. To reduce these effects, RF chokes can be added to certain resistors in the pulse generator electronics. Again, these RF chokes usually result in a slower transition as some of the desired, lower-order harmonics are also attenuated.

3.1.3 Avalanche Transistors

An avalanche transistor is a regular transistor that exhibits avalanche multiplication at high V_{CE}. The mechanism behind the avalanche effect is that under high field, the generated carriers in the collector-base junction have sufficient energy to create additional electron-hole pairs through collision with the crystal lattice. The effect multiplies rapidly once it occurs and the transistor will switch very rapidly [13]. Designing a biploar junction transistor (BJT) to have this property is not well understood. The best method for finding these transistors is to obtain a large quantity of BJTs and test them for the desired avalanche effect.

A typical I-V curve for an avalanche transistor is shown in Figure 3.1.3.1. Operation of the transistor is similar to that of the tunnel diode where the device is biased to a point just before the onset of avalanche breakdown. A trigger is applied which forces the transistor into the breakdown region. Avalanche transistors are used in impulse generators as the capacitance to ground will allow the transistor to

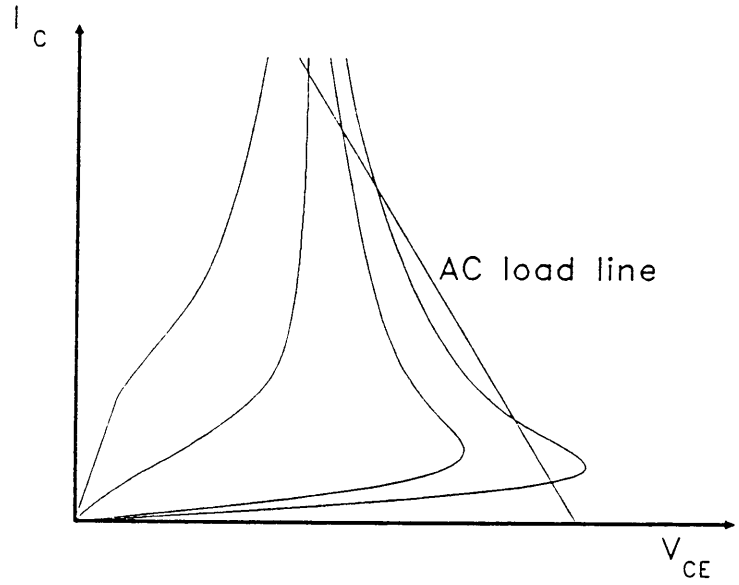

Figure 3.1.3.1 I-V curves for an avalanche transistor [10].

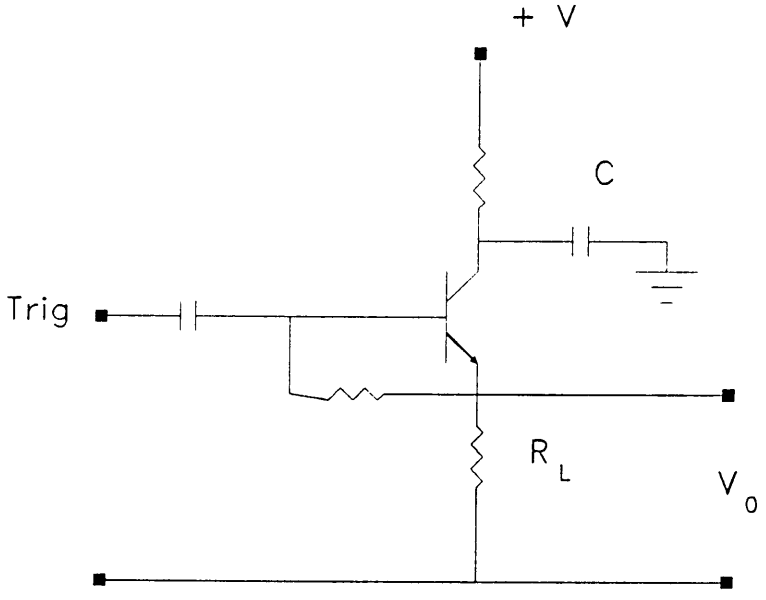

Figure 3.1.3.2 An avalanche transistor impulse generator [10].

reset at the DC Q-point. It is possible to stretch the width of an impulse by adding capacitance, usually in the form of a transmission line, from the collector to ground [10]. A basic avalanche transistor impulse generator design is shown in Figure 3.1.3.2.

The high field required to initiate and maintain the avalanche effect requires that the power supply for such an impulse generator be of the order of 40 volts or higher. Since the TDR specifications limit the power supplies to ± 15 volts, a pulse generator using avalanche transistors was not pursued. Furthermore, it was also estimated that since the sampling window had to be sufficiently wide to allow observation of 100 meters of coaxial cable, a discharge transmission line of equal length would be required to keep the level of the signal at the high level.

3.1.4 Design of the pulse generator

The specifications of the TDR unit made the step recovery diode the choice for the pulse generator. The desire for a high amplitude step pulse precluded the use of a tunnel diode and the limitation of the power supplies prevented the use of an avalanche transistor. Since the SRD is used to speed a transition, a low-speed pulse generator circuit is required. To improve the final waveform cleanliness, a flat-pulse generator was implemented [23].

The flat-pulse generator uses a discrete comparator formed from an emitter coupled pair of microwave transistors. A high speed comparator is used to trigger the discrete comparator. Figure 3.4.1.1 shows the basic schematic for this circuit. The operation of this circuit depends on smoothly switching the current through the

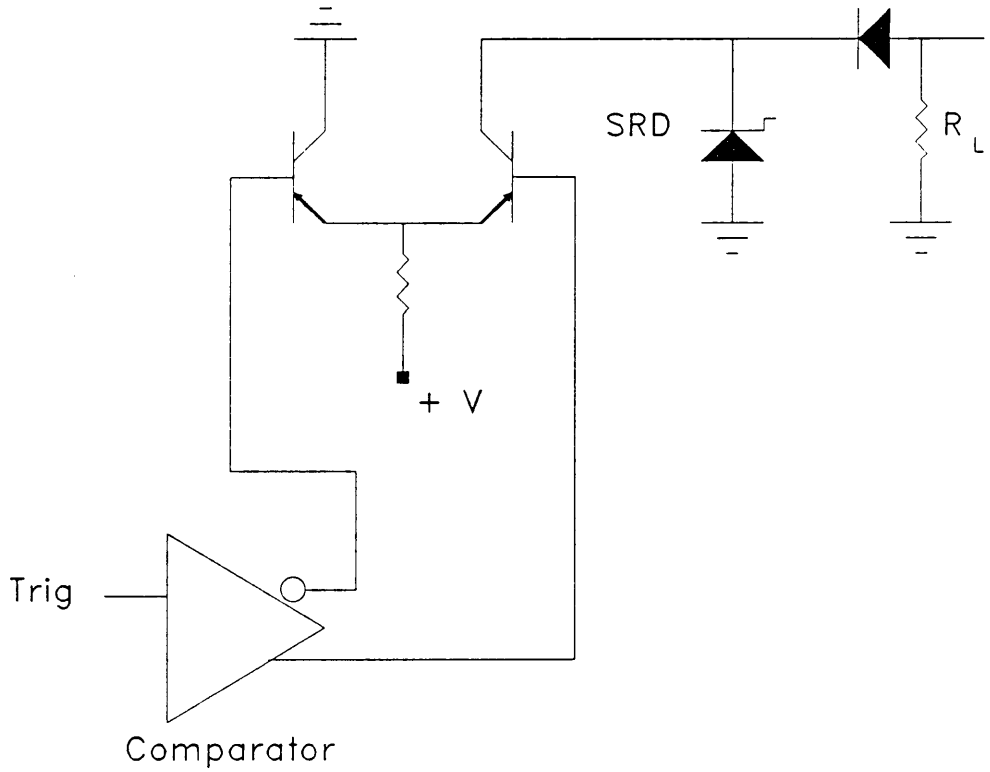

Figure 3.1.4.1 The reference flat pulse generator with SRD [23].

50 Ω load resistors. Normally, the current is at -20 mA resulting in an output baseline voltage of -1.0 volts. When the discrete comparator is triggered, the current, and therefore the voltage, go to zero. The SRD is normally forward biased and switches when the comparator changes state.

Initial results were obtained using a TI 712 comparator, a pair of PNP 3906 transistors and a discrete HP 8032-320 SRD. The resulting waveform had a transition duration of 300 ps. The waveform also had significant distortions, prestep and ringing, as expected. Several changes were made to improve the speed and cleanliness. The comparator was changed to a LT 1016 high speed dual output comparator. The transistors were changed to NEC 88033 PNP microwave transistos and a chip HP 8032-840 SRD was employed. These changes resulted in a transition duration of less than 150 ps. The addition of several Schottky diodes and multiple RF chokes improved the cleanliness of the waveform. Throughout the develoment, changes in component value, package type and manufacturer required constant modification of the design. The dual outputs of the comparator were found to change at slightly different times resulting in large distortions of the output waveform. Later designs use a single output of the comparator to trigger the current switch. The tuning that was performed during this phase had no obvious theoretical explanations. It came to be known as "black magic" where hand selection of components, careful physical placement and a great deal of trial and error testing were required. The final results were within the desired specifications. Figure 3.1.4.2 (a) shows the output of the early testing and (b) shows the result of the modifications and improvements.

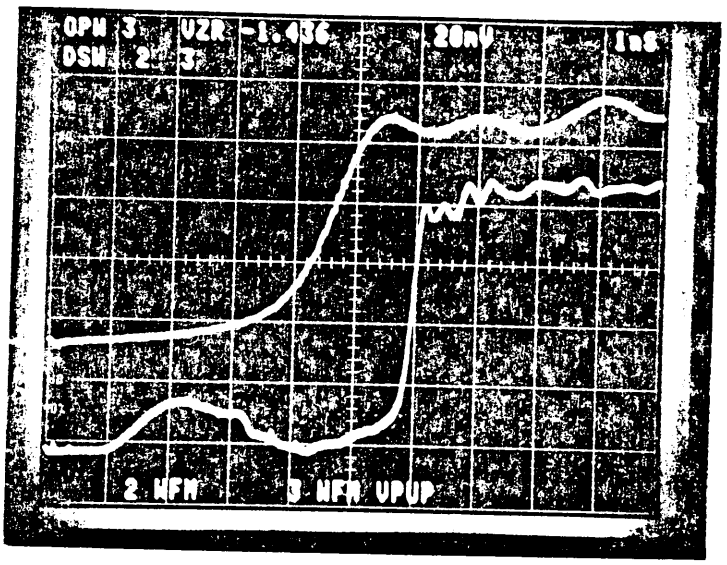

Figure 3.1.4.2 (a) Initial pulse generator output.

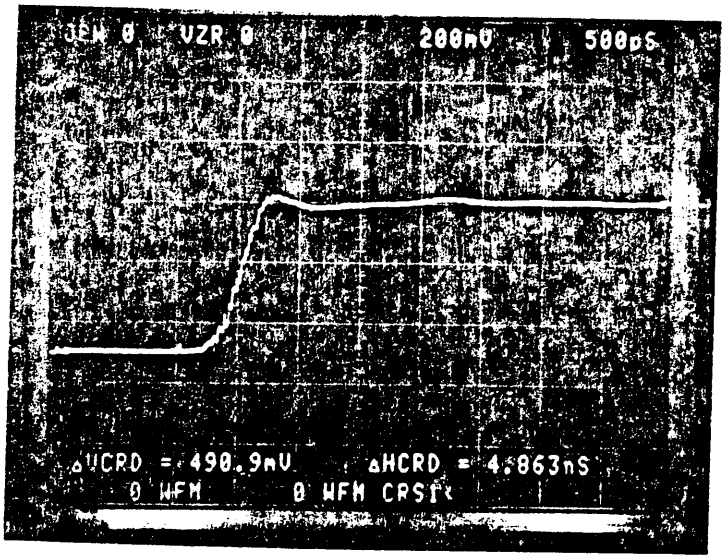

Figure 3.1.4.2 (b) Improved pulse generator output.

3.2 Sampling gate

Because the speed of the TDR signal does not allow direct analog observation, an equivalent time, wideband sampling scheme was used. A small portion of the waveform (sample) is acquired during each repetition of the signal. By incrementing the delay between occurrence of the successive samples of the TDR signal, it is possible to reconstruct the TDR waveform at a slower timescale [3].

A simple sampling gate is shown in Figure 3.2.1. The switches are momentarily closed to allow a small amount of charge to be built up on the capacitor. If the signal being sampled is repetitive, the time the switch is closed can be incremented from sample to sample [14]. By using an integrator, the charge on the sampling capacitor can be converted to a voltage which is proportional to the true voltage on the signal line.

To realize such a system, a pair of diodes are placed on the signal line and biased so both are below their threshold voltage (typically zero volts or reverse biased slightly). A balanced pair of strobes (sampling gate driving pulses) are then applied to both diodes which just turn them on [3,7]. This configuration is shown in Figure 3.2.2. Depending on the magnitude and polarity of the voltage on the signal line, one diode will conduct more than the other. The results in a voltage differential across the sampling capacitors which can be amplified to yield the sampling gate output.

The design of the strobe generator and sampling gate was accomplished by examining existing sampling gate networks [15]. The basic approach is to create a

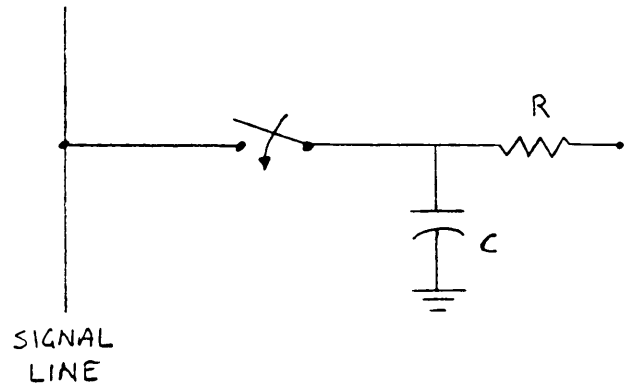

Figure 3.2.1 A simple capacitor sampling gate [15].

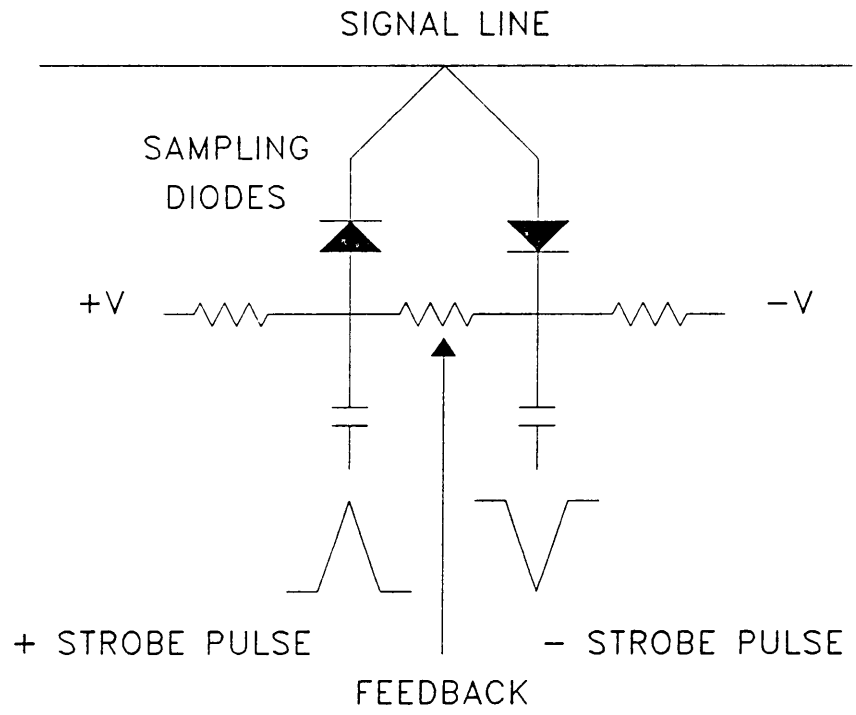

Figure 3.2.2 A 2-diode balanced sampling gate.

narrow triangular waveform to turn the sampling diodes on. To prevent large distortions of the true waveform, the sampling gate must be turned on for a brief instant. The apparent speed of a sampled signal, τ_{sample}, is related to the speed of the true signal, τ_{true}, and the speed of the sampling gate, τ_{gate}, and is given by Eq. 3.2.1.

$$\tau_{sample} = [\,(\tau_{true})^2 + (\tau_{gate})^2\,]^{1/2} \qquad (3.2.1)$$

The technique used to create the narrow strobes is to generate a step pulse using a SRD. This pulse is then sent into a shorted transmission line. The short will yield a reflection coefficient of -1 (see Section 2.1.1) which will force the level back to the baseline. By varying the length of this transmission line, it is possible to regulate the width of the triangular wave such a technique will create. The biasing of the sampling diodes is set to allow only the generated strobes to force the diodes into conduction. This biasing eliminates the need to create a clean pulse from the SRD used in the strobe generator as any ringing is insufficient to turn the sampling diodes on.

The key to developing a sampling gate is to keep the diode bias balanced. Any imbalance would lead to distortion of the sample as one diode would conduct more. To maintain diode linearity and to increase the dynamic range of the sampling gate, the bias on the diodes must be changed after each clock cycle by the amount of voltage sampled. This means that the sampling gate will only sense incremental changes on the signal line and will improve linearity as the diodes are always operating at the same Q-point on their I-V curve [3]. Consequently, the sampling gate output is related to the derivative of the signal voltage. This requires the use of an integrator to yield the proper TDR waveform. The

integration process takes place in the output circuit. Figure 3.2.3 shows the output of the sampling diodes on successive clock cycles and how the bias reset must be accomplished. The circuit used to effect this bias change in the sampling diode bias will be discussed in Section 3.4.

3.3 Timing and control circuits

In the design of this TDR, three timing signals are necessary for proper circuit operation. These are the clock, the slow ramp and the fast ramp. The clock is a 50% duty cycle, 40kHz square wave. The slow ramp is used as the timebase for the equivalent time sampling scheme. The fast ramp determines the sampling window. The amplitude of these two signals should be equal and the key to proper operation of the TDR is to have these ramps be extremely linear.

For this design, a digital slow ramp and an analog fast ramp are generated. The slow ramp is set to 50 ms (τ_{sr}) and is generated once every 2^n repetitions of the clock using a 16-bit digital to analog converter (DAC). The fast ramp is set to 1.2 μs (τ_{fr}) and is generated once per clock cycle. Both signals are positive going and are set to a level of 5.0 volts. The fast ramp is created by charging a capacitor with a fixed current source. The current source is also temperature compensated to minimize nonlinearities. It is also adjustable to allow for adjustment of the fast ramp transition duration.

As mentioned previously, the sampling gate takes a small sample of the signal voltage once per pulse repetition. The next sample is taken at a slightly later point in time. To realize this incremental shift, the two ramps are fed into a high speed

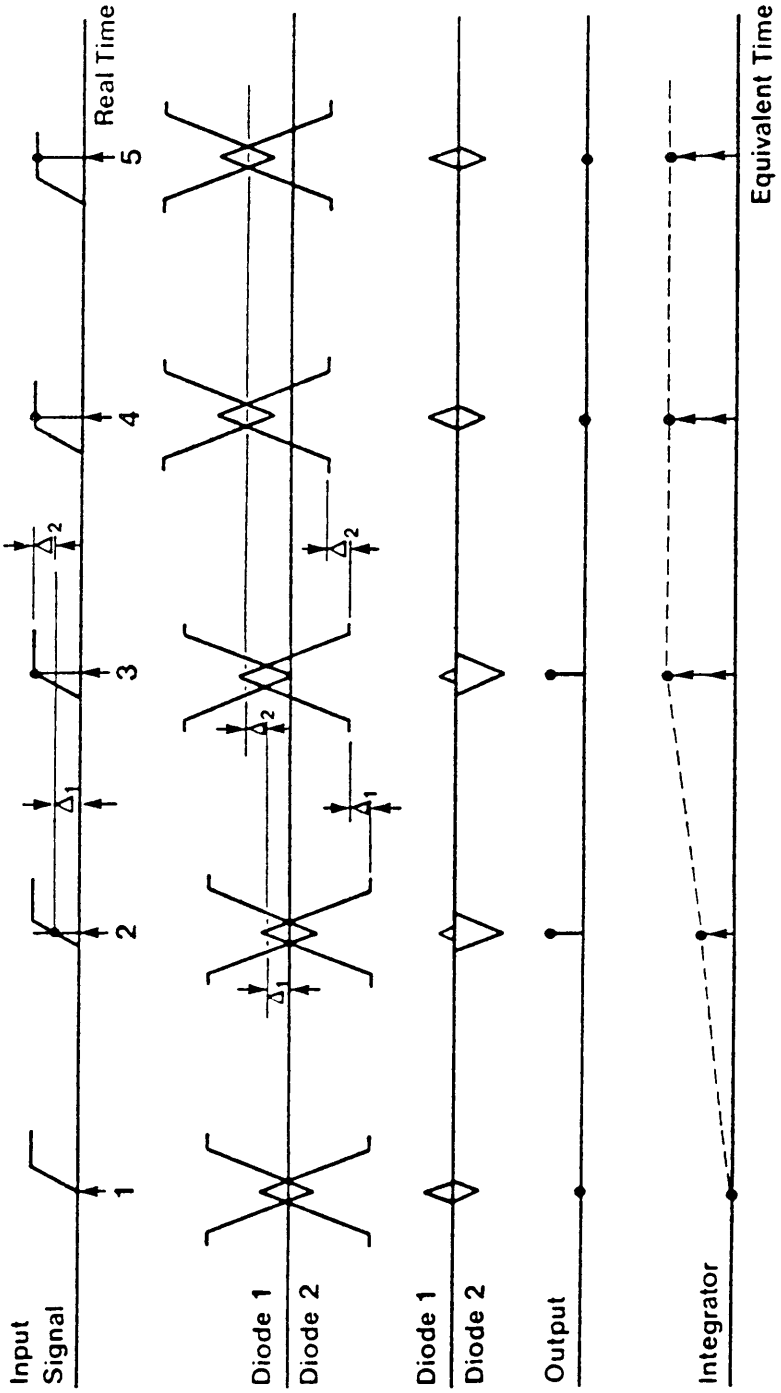

Figure 3.2.3 The effect of bias and feedback shifting with successive samples [3].

comparator. The output of this comparator is used to trigger the strobe generator. Figure 3.3.1 shows the relationship of the two ramps, the true waveform and the sampled waveform. The maximum sampling window is governed by the fast ramp and the sample to sample resolution in time is determined by the number of bits in the slow ramp. The combination being used means that the real time delay between samples is τ_s given by:

$$\tau_s = \tau_{fr} / 2^{16}$$
$$\tau_s = 1.2E\text{-}6 / 65536 = 18.3 \text{ ps}$$

The duration of the equivalent time axis, τ_{et}, is related to the slow ramp by:

$$\tau_{et} = \tau_{sr} / 2^{16}$$
$$\tau_{et} = 50E\text{-}3 / 65536 = 729 \text{ ns}$$

3.4 Output and feedback circuit

The output circuit takes the incremental voltages from the sampling diodes, amplifies them, and then integrates the voltage over the sampling period. Feedback from the integrator is then used to shift the bias point of the sampling diodes to the voltage level of the previous sample. This insures that the diodes are not damaged due to large voltage changes from sample to sample and also allows the gate to perform over a wider signal voltage range.

To insure that the integrator only operates during the sampling period, a second sampler is used. This circuit is an FET gate which is placed between the

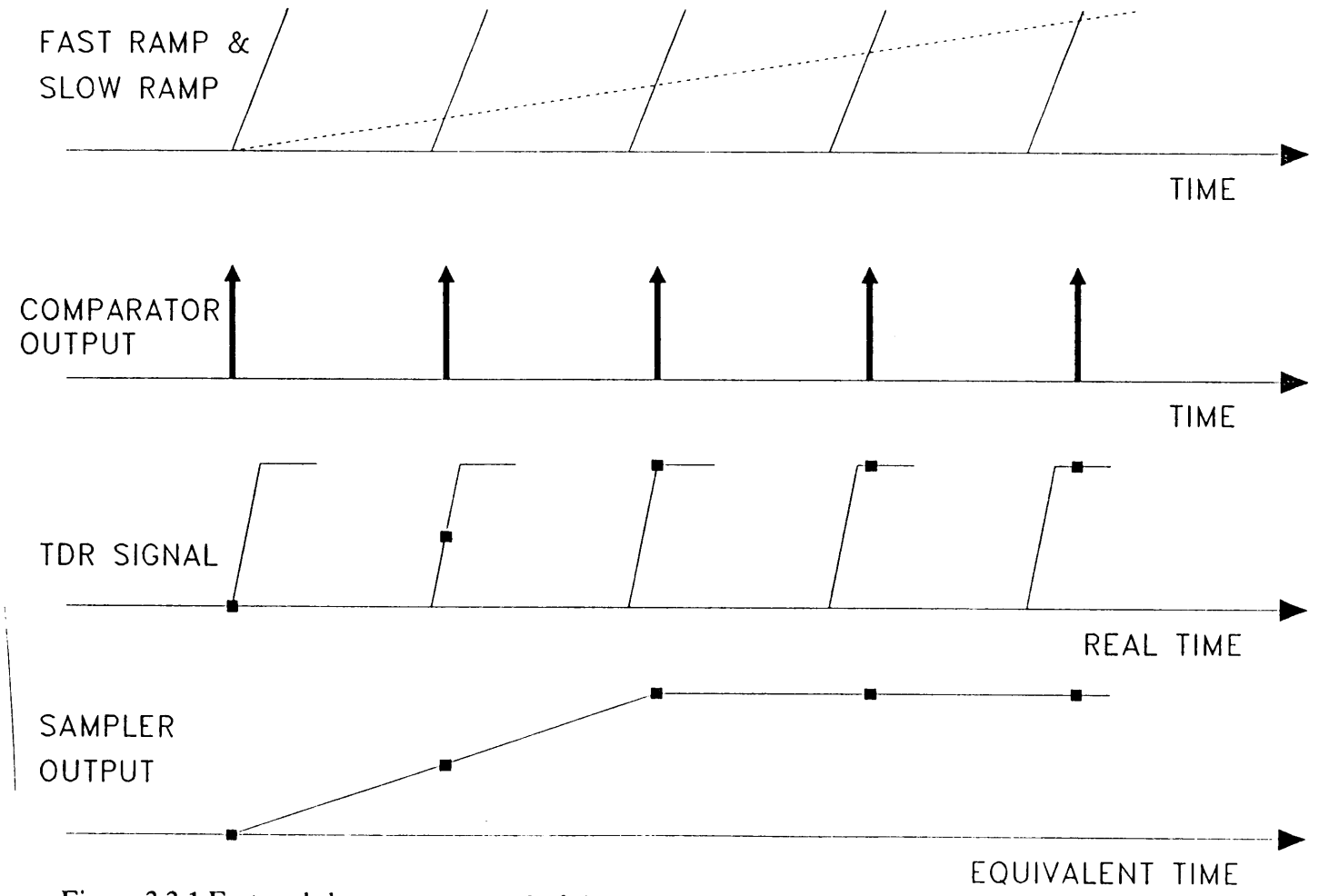

Figure 3.3.1 Fast and slow ramp control of the sampling gate and the sampling gate output.

amplifier and integrator. When the sampling gate is turned on, the FET allows the signal to pass to the integrator. The control signal fed to the FET is generated from the slow ramp/fast ramp comparator output and is adjusted by a one shot multivibrator [7]. The amplifier in the output circuit is necessary as the voltages coming from the sampling gate are very low. The total loop gain to the output circuit also insures that the sampling gate can correctly operate through the entire range of TDR voltages.

Chapter 4

Thick-Film Technology

4.0 Introduction

In this chapter, thick-film processing and materials technology will first be described in general. Specific requirements, limitations, problems and techniques for using thick-film technology at microwave frequencies will then be covered. Special considerations required in the design of the TDR will be addressed as well as a design process which can be applied to any hybrid design.

4.1 Thick film processing

This section will detail the thick film process steps necessary to create a hybrid

electronic circuit. Emphasis will be placed on certain aspects of the process which might affect the microwave characteristics of the final circuit.

Thick film printing is little different from standard silk-screen printing techniques. A pattern is created in a stainless steel screen through which paste is forced onto a ceramic substrate. The paste is then treated to yield desired mechanical and electrical properties. Further printings may then be added to yield a variety of electrical components. Thick film printing is capable of realizing all passive circuit elements such as resistors, capacitors and inductors as well as all conductive interconnects. Thick film has a special advantage in its ability to allow the printing of conductive crossovers.

In thick film printing, each component type: resistor, capacitor, inductor, etc. require a separate printing and therefore a separate screen. Each screen will contain the desired shapes dictated by the design. Certain paste types require the use of different kinds of screens. The variation from screen to screen is the number of openings per linear inch. This is called the mesh count and affects the minimum line definition of the printing and the quality of the deposited paste. In simple terms, the higher the mesh count, the finer the line definition that can be obtained [16]. The deposited paste is also affected by the mesh size as a higher mesh count also reduces the probability of pinholes which are regions where air bubbles in the mesh inhibit the deposition of paste.

In this work, the screens were made by placing a photosensitive emulsion on the mesh. An actual size, negative image of the desired pattern was created by photographing a high-contrast (Rubylith®) positive. This positive was reduced ten

times during this process. The Rubylith pattern was generated using a computer-aided design package (CAD) called MicroCAD and plotted with a Optical Computer 9875 pen plotter and a Micrasem model MP-1 diamond tip scribe. Once the negative was made, it was placed on the emulsified screen. The screen and negative are then exposed to ultraviolet (UV) light which hardens the emulsion in all areas except for the pattern regions. The pattern is then washed out as the unexposed emulsion is water soluble. The screen is then dried and is ready for the printing process.

The actual printing was done on a AMI Presco Model 465 and Model 685 semiautomatic screen printer. The printer allows for proper alignment with the substrate and any previous printed patterns. This control is accurate to about 0.5 mils. Once the screen is mounted in the machine and the substrate positioned properly with respect to the pattern in the screen, several adjustments are made which will affect the print quality. The most important adjustment is the snap-off or breakaway distance. This distance is measured from the surface of the substrate to the underside of the screen. It is a critical parameter in the printing process for several reasons. Some snap-off is required to prevent the pattern from being smeared after printing is complete. Snap-off will also affect the printed thickness and line resolution.

Another critical adjustment is the pressure of the squeegee blade which forces the paste through the screen. These pastes have a complex viscosity characteristic which is known as thixotropic viscosity. At rest, the paste has a high viscosity which prevents excess paste from oozing through the screen. The rest high viscosity also means that the printed pattern will not spread over the substrate but will retain the

desired pattern. During the actual printing process, the squeegee blade moves the paste over the entire pattern region. The thixotropic nature of the paste means that during motion, the viscosity is relatively low which makes it possible to force the paste through the screen. The speed of printing and the pressure exerted by the squeegee on the paste will both affect the print quality.

Once the printing is complete, the substrates are allowed to sit in a room temperature environment for 10 to 15 minutes. This allows the surface of the paste to settle slightly which makes this surface smoother. This is of importance if further printing requires that pastes be printed on top of each other. If the surface were not allowed to settle, the impression of the mesh would be left in the print and would lead to problems in retaining line definition in later printing. After settling, the substrates are placed in a 150° C Blue-M drying oven for 15 minutes. This oven is used to evaporate the organic solvents used in the paste to which give the paste its thixotropic nature. The low temperature of the oven insures that all of the solvents will evaporate prior to formation of a gas impermeable layer on the printed paste. Once the drying is complete, the substrates are then moved to a multiple temperature zone BTU model VPI-1 furnace. The furnace has a moving nichrome belt on which the substrates are placed. The speed of the belt and the temperature of each zone is fixed such that the substrates go through a specific heating and cooling profile. The particular settings will vary according to paste manufacturer and paste type. It is this high temperature cycle that determines the electrical properties of the printed paste.

Once the full cycle is complete, the substrates are then ready for further printing or can go to final component attachment and testing. If multiple printed

layers are required, the layers must be printed and fired in a certain order to yield the desired results. This is necessary as certain types of paste will change electrical properties if they are subjected to repetitive furnace treatment. Specifically, resistors will typically change in resistivity and the temperature coefficient of resistance (TCR) will also increase [16]. Dielectric material used in forming either crossovers or capacitors will show an increase in the relative dielectric constant. It is therefore necessary to fire all resistors simultaneously and to fire them as the last printed components.

Once all components have been printed and fired, it is possible to attach active devices; diodes, transistors, monolithic integrated circuits, etc., to the thick film substrate to form a complete hybrid electronic circuit. This is how the term "hybrid" was coined. The final circuit is a hybrid using more than one processing technology. In this case, thick film printed components and discrete monolithic devices. This component attachment is accomplished in one of two basic ways; either to solder components onto printed metalization or to adhere these components by using conductive epoxy. The choice of these two techniques depends on the device manufacturer. Current trends in the semiconductor industry seem to favor surface mount components which are soldered to the substrates. The advantage of this kind of package is that there are no exposed wirebonds which are necessary if the semiconductor chip itself is used. This also reduces the amount of labor required as wirebonding requires direct human control. It is also possible to attach surface mount chip resistors, capacitors and inductors if a high tolerance is required on these components. While it is possible to trim printed components to extremely tight tolerances, $\leq .1\%$, doing so can take a large amount of time if there is no automated trimming equipment available. The reason trimming is required is due to the

variation in printing thickness from print to print as well as variations in the furnace profile. Both of these problems force the hybrid designer to require trimming if the high tolerance is required. In the case of resistor and dielectric paste, the electrical characteristics of these materials depend on the thickness of the print. Since the control over printing thickness is difficult, most process lines must be self-tested regularly to give the best estimate of what the final values will be. These values can then be used in the design phase to reduce the amount of trimming that must be allowed for. In an uncorrected case, resistors are typically designed to 80% of nominal and capacitors are designed to 120% of nominal. In a well known environment, it would be possible to get these values to within 10% of nominal.

4.2 Thick-film Considerations at Microwave Frequencies

The preceding section described the thick-film process in general. This section will address the problems that can be encountered when using thick-film technology at microwave frequencies. These considerations affect the design of the hybrid circuit as well as the processing steps.

Thick-film techniques have several advantages when used to fabricate high frequency circuits. Specifically, conductor patterns are short which minimizes path resistance and parasitic inductance. Conductor materials such as gold can be used to further decrease the path resistance. Substrate materials have a low dielectric (ϵ_r) constant which helps to reduce the parasitic capacitance between conductor runs and mounted components. It is possible to print a ground plane on the reverse side of the substrate to further reduce capacitance. Finally, most mounted components have short leads and low packaging capacitance [16].

4.2.1 Substrates

There are two basic requirements that must be satisfied in the selection of a substrate material for use at high frequency: low dielectric constant and uniform material properties. The three most common ceramic substrates used for high frequency fabrication are alumina, steatite and beryllia. Each of these substrates has a number of advantages and disadvantages which will are listed below [16,17].

Alumina (96%)

-Relatively high ϵ_r (8.5 - 10 @ 1MHz)
-High physical strength
-Good thermal characteristics
-Low cost
-Relatively rough surface
-low loss tangent

Alumina (99.5%)

-Similar to 96% alumina
-Higher cost
-Good surface smoothness
-Lower material property variation

Beryllia

-Low ϵ_r (6.0 - 6.5 @ 1MHz)

-High thermal conductivity, good for high-power applications

-Low physical strength

-High cost

-Highly toxic in powdered form

Steatite

-Low ϵ_r (5.5 - 6.5 @ 1MHz)

-Poor physical strength

-Poor thermal properties

-Poor compatibility with noble metal materials (Au, Ag, AgPd)

In addition to these characteristics, the processing steps in manufacturing the substrates can affect their high frequency performance. The density variation of the substrate will affect the dielectric loss over the entire area. Surface finish of the substrate will determine the minimum line resolution and can distort the surface of the printed material. Chemical purity will affect the dielectric constant and the loss tangent of the substrate.

For the soil moisture TDR application, 96% Alumina was used because of the lower cost of the material. To overcome the higher dielectric constant of this material, several iterations of the design were performed to find the optimum

placement of components when parasitic capacitance was found to be a problem.

4.2.2 Conductor Materials

The main requirement for conductor materials is high conductivity to reduce the series resistance of interconnects. Line resolution is of secondary concern and most currently available thick-film conductor pastes can be printed with a resolution of less than 5 mils (0.005 inches). Other characteristics a conductor material should have include: solderability for mounting components, compatibility with ultrasonic and thermal compression wirebonding, low cost, high substrate adhesion and low metallic ion migration into printed resistors and capacitors [16,18].

From the consideration of high conductivity alone, pure silver (Ag) or pure gold (Au) are the best conductor materials. However, neither material is usable if soldering is going to be performed. Silver has a tendency to migrate into printed resistors which reduces the resistance value. For these reasons, silver-palladium (AgPd) paste was used despite having a much higher sheet resistance (ρ_s). Typical values for ρ_s for Ag and Au are between 1-5 mΩ/□ and for AgPd are between 20-40 mΩ/□ [19]. The disadvantage of AgPd was overcome by placing critical components as close together as possible. Another possible solution which was not explored would be to overprint the AgPd with pure silver or gold to improve the performance.

4.2.3 Resistor and Dielectric Materials

In the TDR design, printed resistors and capacitors were not used to eliminate

the trimming normally required of these components. Furthermore, crossovers were avoided in the design to reduce the parasitic capacitance these structures cause and to reduce the number of printing operations. However, a brief overview of these materials and their high frequency characteristics is presented.

In general, highly-resistive materials will tend to decrease in value while lower resistivity materials will tend to increase in value with increased frequency [16]. Resistor shape will also affect the performance. A square resistor exhibits the best performance while a resistor with an aspect ratio less than 1 will show the poorest performance. If printed resistors are to be used, it would be best to trim these resistors to their nominal value while being tested at the operating frequency. Most trimmer systems perform a DC trim which would not yield the desired high frequency value of resistance.

Printed dielectric materials behave well over a wide frequency range. Printed capacitors are often preferred for this reason but usually space limitations prevent their use. Chip capacitors with ceramic or porcelain dielectrics are good substitutes for printed capacitors as they do not have long leads which cause parasitic inductances. As mentioned previously, crossovers are to be avoided when designing microwave hybrids but if they must be used, a low ϵ_r dielectric material like DuPont 5704 (ϵ_r = 9 @ 1GHz) [20] provides adequate performance. It is recommended that any unavoidable crossovers be placed between power supply lines and ground lines. This will increase the decoupling of the supplies.

4.3 Design Requirements for the TDR

The hybrid version of the TDR unit was originally designed to be fabricated on two 1" x 2" 96% alumina substrates. This specification was based on the possible need to place the TDR unit within the ground probe used in the soil moisture measurements. All of the TDR subsystems would be placed on the two substrates with the exception of the slow ramp generator. For flexibility, the pulse generator, sampling gate and fast ramp circuits were all placed on one substrate and the output/feedback circuit was placed on the other substrate. This made for a more flexible TDR unit as the pulse generator, sampling gate, fast ramp or TDR impedance could be changed but the same output circuit could be used irregardless of these modifications. Thus if a 75Ω TDR system or an impulse pulse generator was required in a later application, only one substrate need be modified. As the design progressed, it was decided that 1" x 3" substrates were necessary to accommodate later circuit additions and to provide for greater ability to control discontinuities on the TDR coplanar transmission line.

As the TDR system is a commercial product, manufacturing considerations affected the design requirements. As mentioned previously, trimming of passive components is time consuming so surface mount chip versions of all passive components were to be used. To reduce the printing time and improve the microwave performance, crossovers were eliminated when the 1" x 3" substrates were used. Component placement was found to be critical in the pulse generator and sampling gate subsystems and the speed with which a hybrid circuit can be modified was of particular use. The basic requirement for the circuit was to keep all high frequency, low signal level conductor runs as short as possible.

4.4 Design Approach and Results

Each substrate was designed separately according to the following procedure. First, the electronic schematic was redrawn to show all interconnections necessary while using the actual device package outlines. This allowed for seeing where crossovers were necessary and the possibility for their removal. Crossovers were usually removed by running conductors under the packaged devices, chip resistors and chip capacitors. Where this was not possible, power supply crossovers for example, the power supplies were split and connected together off of the substrate. Figure 4.4.1 shows the schematic for the original output circuit. Figure 4.4.2 shows the same schematic redrawn with the actual packages used.

Once the crossovers were eliminated, the modified schematic is transferred to a hybrid conductor layout. At this time, space and microwave considerations were addressed. In particular for the output circuit, the signal coming from the sampling gate is a low level, high frequency signal so the distance from the substrate edge to the input of the buffer was minimized. Similarly, the distance to the AC amplifier was also reduced to help prevent the signal from being distorted or attenuated by the high resistivity AgPd paste. Also, the nominal conductor width for all of these signal lines was 20 mils. After the amplifier, the normal microwave problems are not as apparent. The signal in this section of the TDR is of lower frequency and of such high amplitude that conductor run length was not a great concern for the rest of the substrate. Although thermal problems were not expected with the output circuit, the amplifiers were spaced to evenly dissipate any heat generated.

The pulser/sampler substrate required more care in the physical layout. The

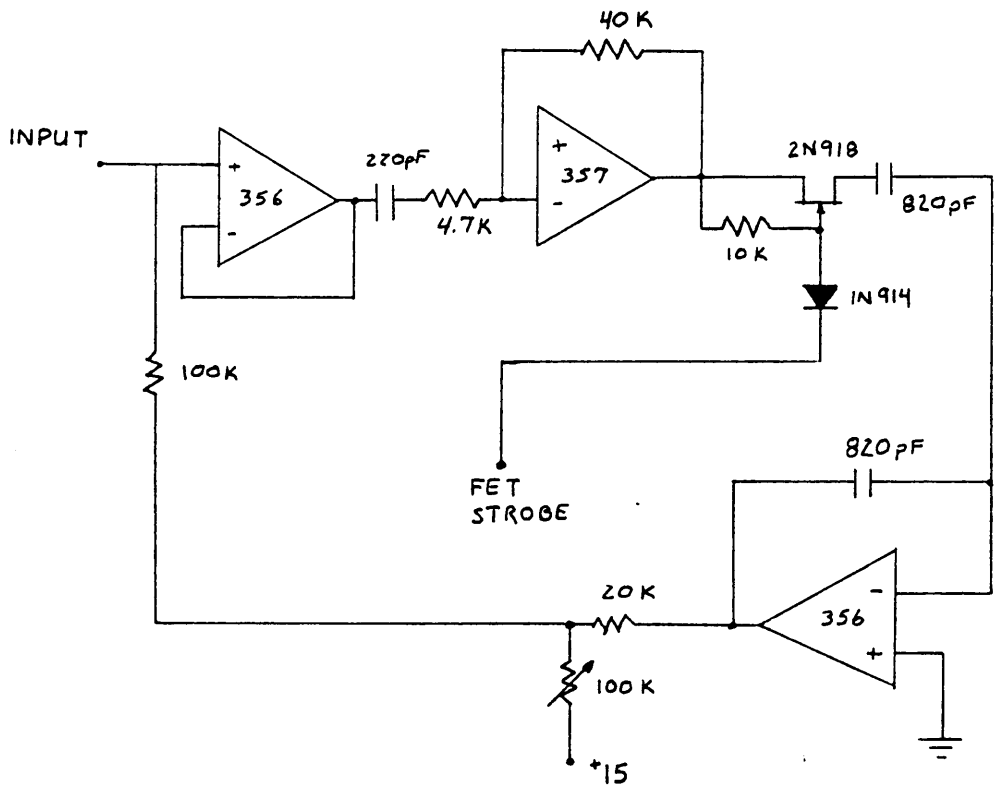

Figure 4.4.1 The original output circuit schematic.

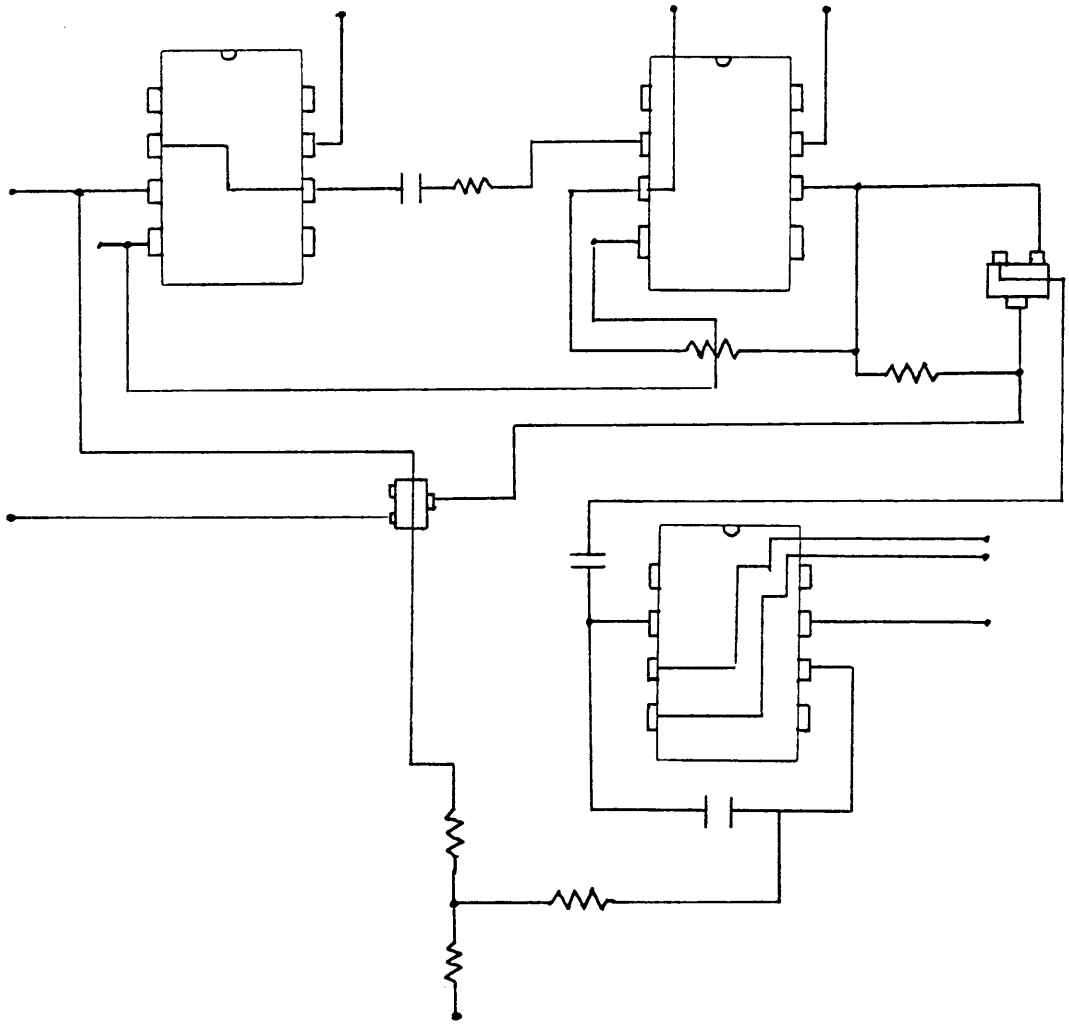

Figure 4.4.2 The output circuit redrawn with package outlines.

initial removal of crossovers was performed in the same way as the output circuit. More care was taken in the pulser and sampler sections. The pulser was designed to have the distance between each of the cascaded electronics be as small as possible. Furthermore, the signal flow required that the step recovery diode be as close to the transmission line as possible. This was necessary as the high speed components of the sharpened pulse would have been attenuated and radiated in any conductor that was not a transmission line structure. The sampling gate and strobe generator was designed for maximum symmetry to insure that the strobes would be balanced. Since the strobe generator relies on a pair of balanced shorts to create the triangular waveform, these were built into the ground plane of the coplanar line. The rest of the strobe generator was placed about the center line of the shorts with the distance to each component being kept equal. As with the output circuit, thermal problems were not accounted for in the initial layout but were later revisions did require spacing of components to reduce self-heating problem which led to performance variation. In particular, the fast ramp generator was moved farther from the microwave transistors and the high speed comparators to help reduce thermally induced nonlinearities. Also, the levels of the fast and slow ramps were changed to 4.0 volts to reduce heating of the LT1016 high-speed comparators.

The design approach worked quite well for the TDR application. With the emphasis on eliminating crossovers, it was relatively easy to achieve a good initial high-frequency design. As the TDR systems were tested, specific changes were required in component placement that could not be deduced from the schematic. In particular, the initial designs used step recovery diodes in chip form. These were attached to the substrate with conductive epoxy. Due to the high dielectric constant of the alumina substrate, there was significant parasitic capacitance between the

SRD and other components which appeared as ringing in the generated pulse. Later designs first called for moving the SRD to minimize these effects and eventually, the chip form of the SRD was replaced with a beam leaded device. The advantage of this sort of package was that the SRD was suspended above the substrate by the leads which greatly reduced the parasitic capacitance effects.

Another area of the design where modifications to the initial design were required was the coplanar transmission line itself. The dimensions of the center conductor, gaps and ground plane width were based on known experimentation [21]. These values were altered slightly due to the characteristics of the DuPont 6134 AgPd paste used in printing the conductor metallization. In addition, the packaging capacitance of the sampling diodes created a discontinuity which appeared as part of the generated TDR pulse. To counter this local capacitance, the ground planes were widened and the center conductor narrowed in the region where the sampling diode package contacted the transmission line. Additionally, the gap was again increased around the blocking capacitor placed in the center conductor and at the edge of the substrate where a coaxial line is attached. If these discontinuities were left uncorrected, their effect would be to distort the TDR waveform and could lead to errors in interpreting the TDR response.

Chapter 5

Test And Calibration of the TDR

5.0 Introduction

This section will give a detailed listing of the proper procedures for tuning the individual TDR subsystems and will include waveforms or properly and improperly tuned units. Comparisons will be made between the actual waveforms and the results of the Pspice modelling. The performance of the system will also be compared to several commercial TDR units with emphasis on signal level, waveform cleanliness and transition speed. A system timing diagram showing the relationship of all generated signals is given for reference in Figure 5.0.1.

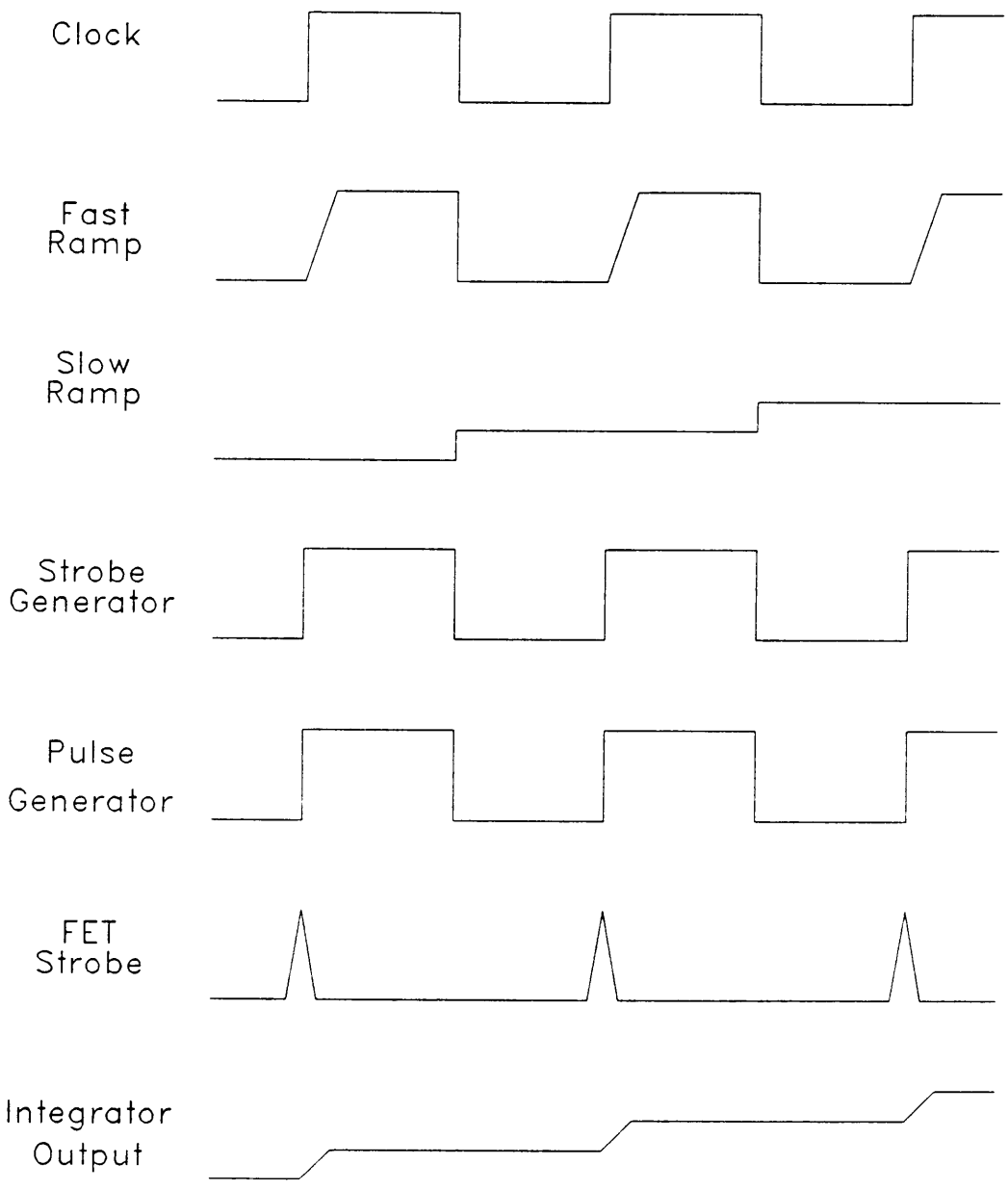

Figure 5.0.1 TDR system timing diagram of control signals.

5.1 Test Points and Procedures

The circuit schematics for the subsystems are shown in Figures 5.1.1, 5.1.2, and 5.1.3. The test points mentioned in the text are indicated. Each of the tests is preformed using a Tektronix 7854 mainframe oscilloscope, 7S12 Sampling module, S-4 Sampling head, S-53 Trigger recognizer, 7A26 Dual trace vertical amplifier and 7B53A Timebase. Each test will indicate any special triggering or probe attachment as necessary. Several of the tests are performed on individual subsystems and others are performed to verify the TDR operation as a whole unit.

5.1.1 Pulse Generator

The pulse generator is tested using the S-4 sampling head in conjunction with the 7S12 sampling module. The purpose of this test is to set the level of the pulse generator, to measure the transition speed and to observe the waveform cleanliness. In order to properly trigger the S-4 sampling head, one of two approaches may be used. Either the clock signal is fed through a variable delay generator with the pretrigger connected to the S-53 trigger recognizer and the main trigger connected to the clock input of the substrate or the same clock signal can be sent to both the substrate and the S-53 and the delay potentiometer (P2) of the pulse generator itself can be used to place the pulse in the S-4 sampling window. Since the latter technique disturbs the substrate the least, it is the one of choice. Figure 5.1.1.1 shows the proper connection of the substrate to the test equipment. It does assume that the generated pulse attributes do not change over the delay range allowed by the delay potentiometer. Testing has shown that this is a good assumption.

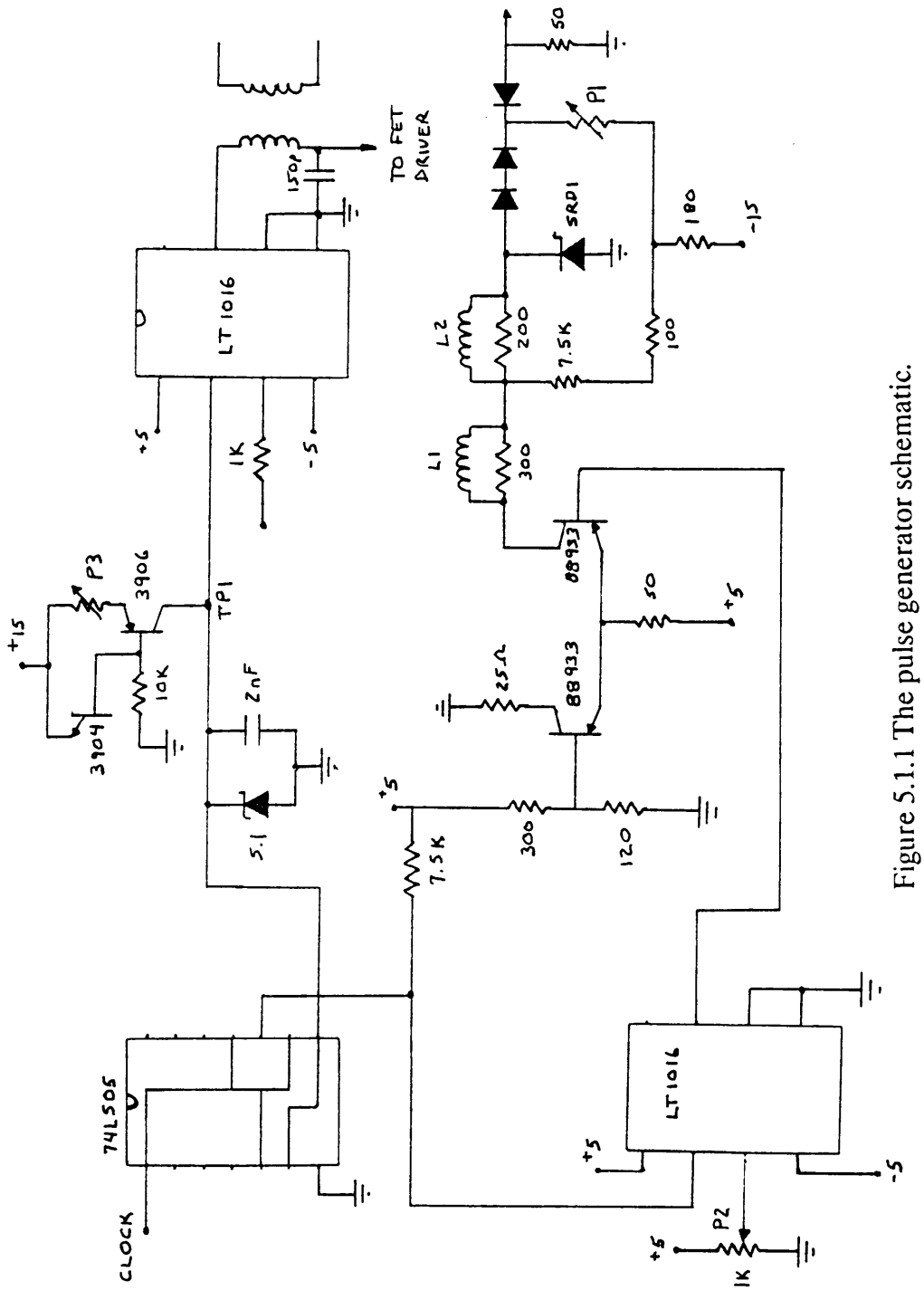

Figure 5.1.1 The pulse generator schematic.

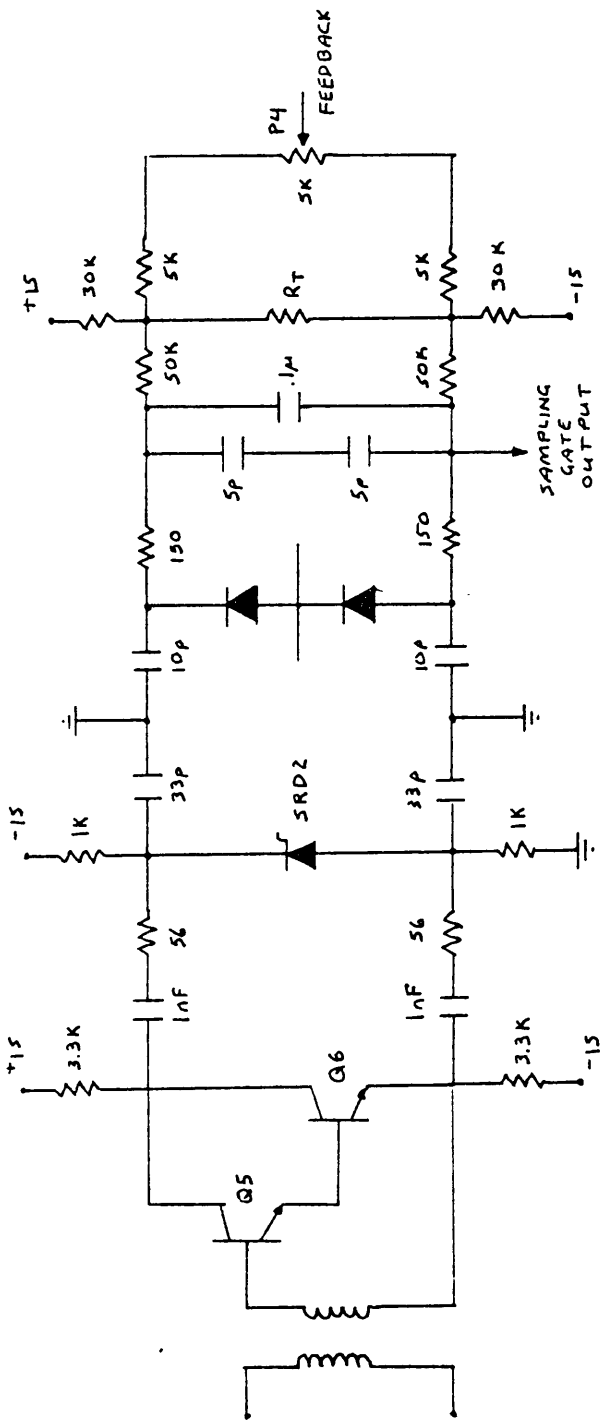

Figure 5.1.2 The sampling gate and strobe generator schematic.

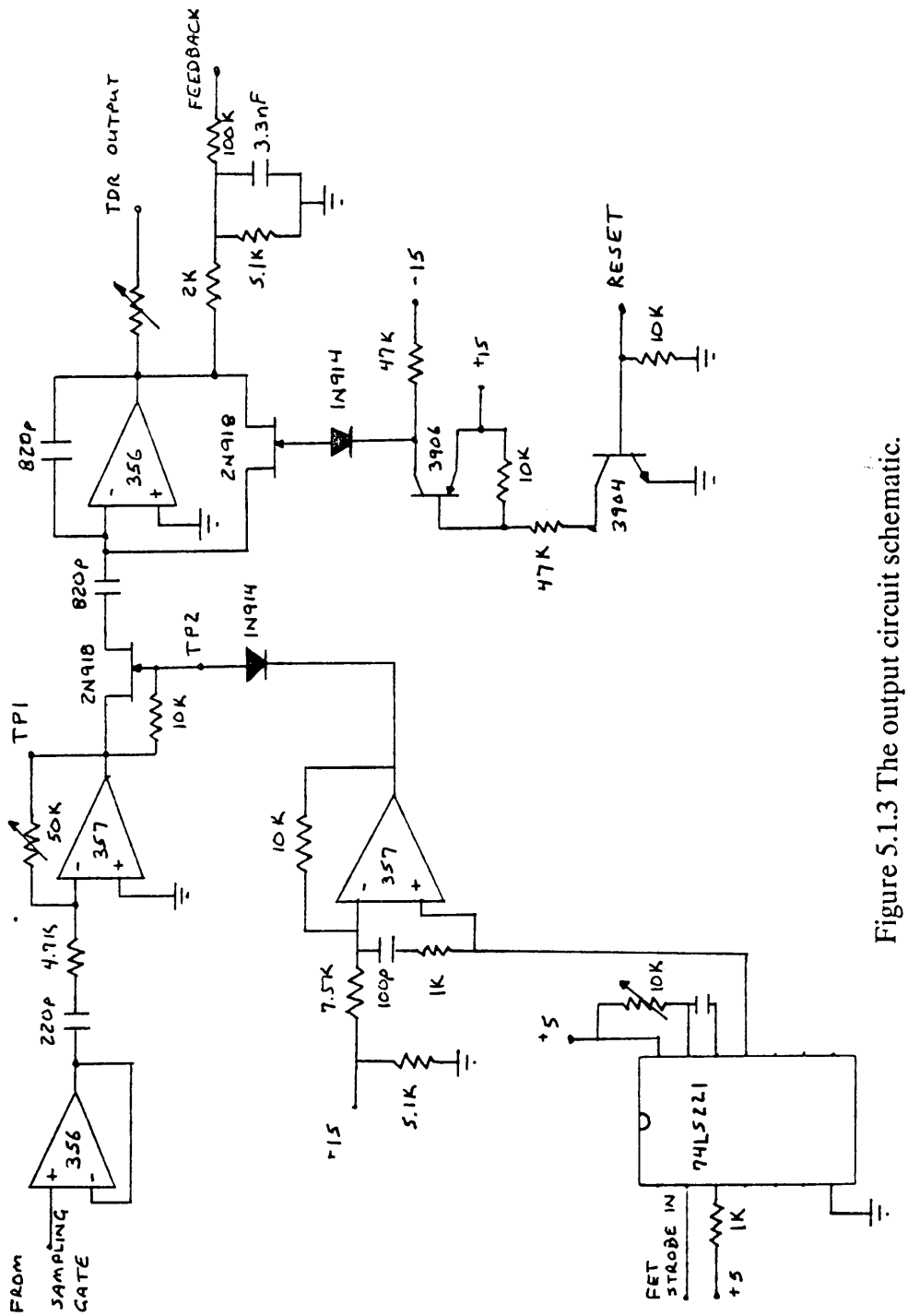

Figure 5.1.3 The output circuit schematic.

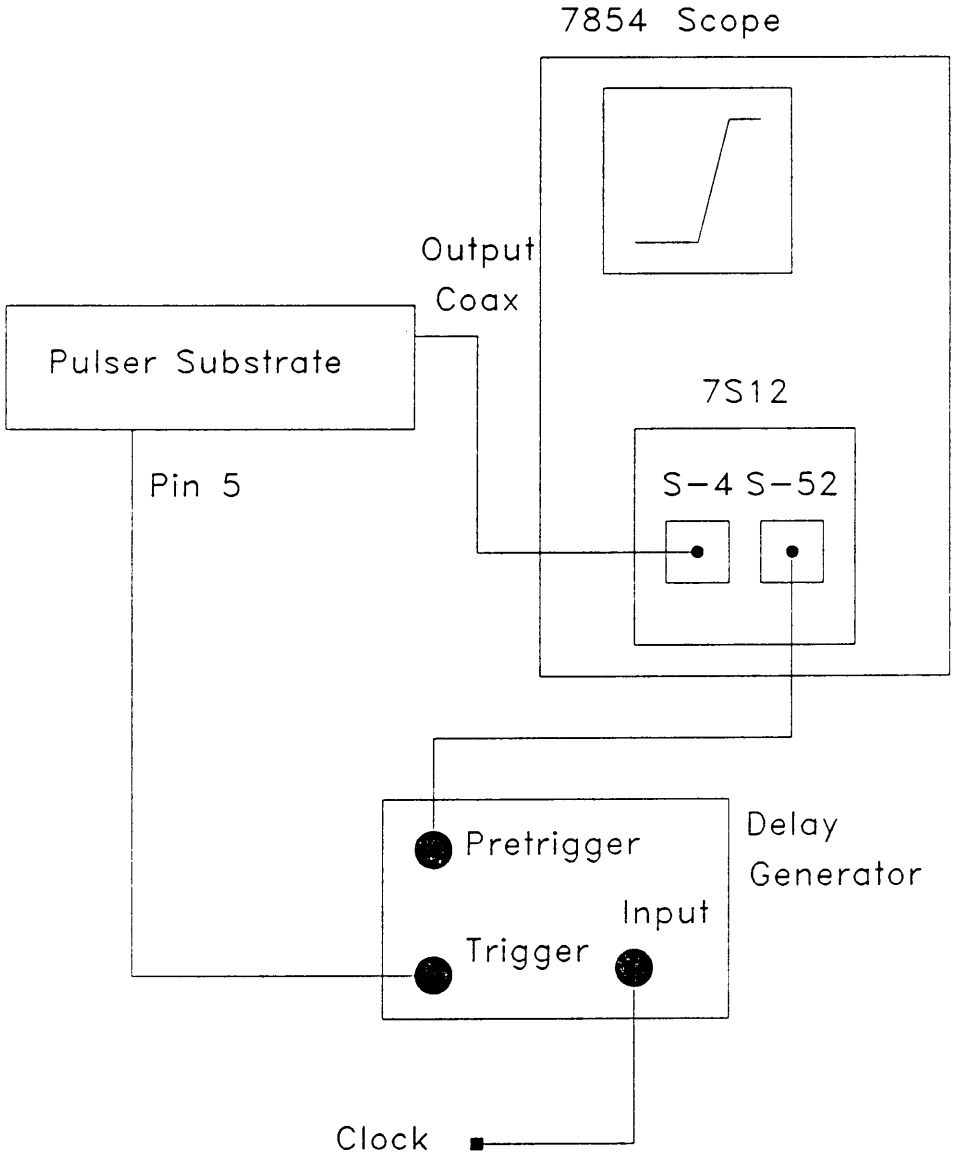

Figure 5.1.1.1 Delay generator connections for observing the pulse generator output.

Once the pulse is observed in the S-4 display, the pulse amplitude potentiometer (P1 of the pulser schematic) may be adjusted to yield an amplitude of 0.6 volts. The S-4 has an input impedance of 50Ω and the desired amplitude of the pulse generator is 0.6 volts into such a load. The modifications of the pulse generator (Schottky diodes and RF chokes) mentioned previously should already be acting as intended. Occasionally, it is necessary to physically adjust the RF choke coils to a particular spacing to reduce ringing. It is also necessary to select the values of resistors R6 and R3 for proper operation of the SRD. The variation of individual SRD chips necessitate this hand selection. In some instances, the LT1016 (U3) itself had poor performance and occasionally, these had to be replaced.

5.1.2 Fast Ramp

The fast ramp required only minor adjustment of the current source potentiometer (P3) to insure the transition duration was 1.2 μsec. A check can also be performed to insure good linearity from 0.5 to 4.5 volts as the linearity of the fast ramp is the key to insuring accurate sampling (linear display time axis). The test point for the fast ramp is TP1. Figure 5.1.2.1 shows the proper fast ramp generator output.

5.1.3 Output Circuit

There are two tests that need to be performed on the output circuit and these are documented in order. The adjustments made are only to produce roughly correct performance which will then be fine tuned when the whole TDR system is tested.

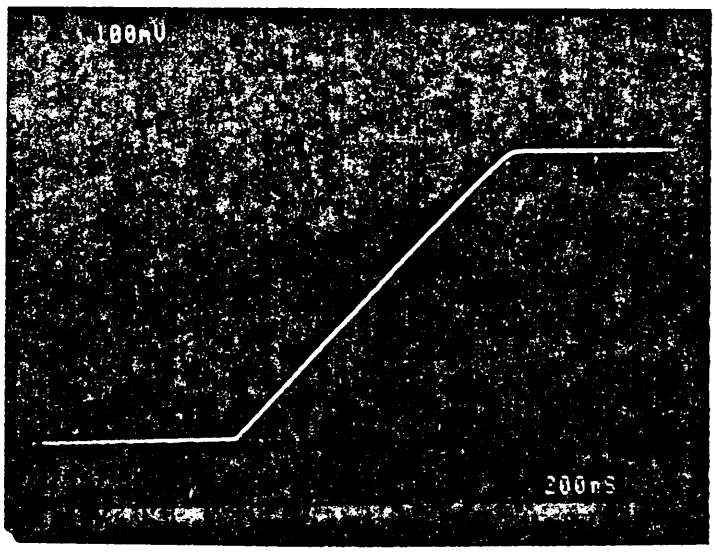

Figure 5.1.2.1 Correct fast ramp output.

The first test is to set the amplifier gain. By placing a scope probe at TP1 of the output circuit schematic, the amplifier output can be observed. Figure 5.1.3.1 shows a correct output. The second test is performed by observing the waveform at TP2. This is the second sampler width adjustment and controls the integrator sampling period. This test may be done without an FET scope probe and yields an output shown in Figure 5.1.3.2. Once these two tests have been finished, the TDR unit should be operating well enough for final fine tuning.

5.1.4 Final Tuning

The final tuning will set the gain of the output circuit, second sampler gate width and feedback balance. The TDR waveform should be observed at pin 17 of the output circuit and the slow ramp should be used to provide the horizontal timebase. There should be a 2 foot piece of coaxial cable attached to the coplanar line of the pulser/sampler substrate.

The first adjustment should be made to the second sampler width. Observe the last few samples of the end of the TDR waveform and the first few at the beginning of the next repetition of the waveform. There should be an abrupt jump from the high level of the preceding TDR waveform to the baseline of the new waveform. Figure 5.1.4.1 (a) shows the case of oversampling, (b) shows the proper adjustment and (c) shows undersampling. The second sampler potentiometer (P3 of the output circuit) should be adjusted to yield the proper response. The feedback potentiometer (P4 of the pulser) should be adjusted to make the amplitude of the reflected pulse equal to that of the initial pulse. Once this is correct, the gain of the amplifier in the output circuit should be adjusted as the termination of the

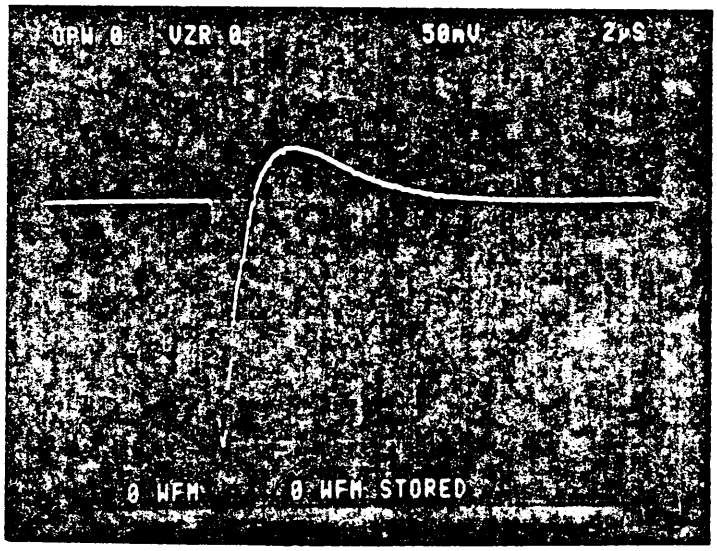

Figure 5.1.3.1 Correct amplifier output in the output circuit.

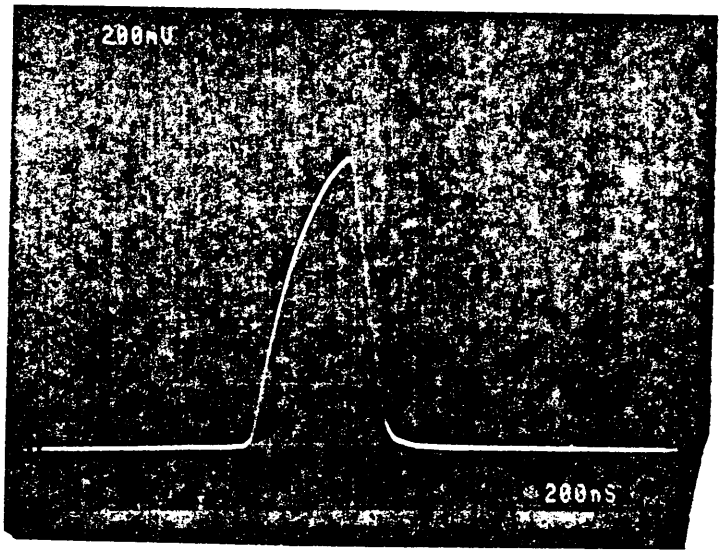

Figure 5.1.3.2 Correct FET strobe observed at the FET gate.

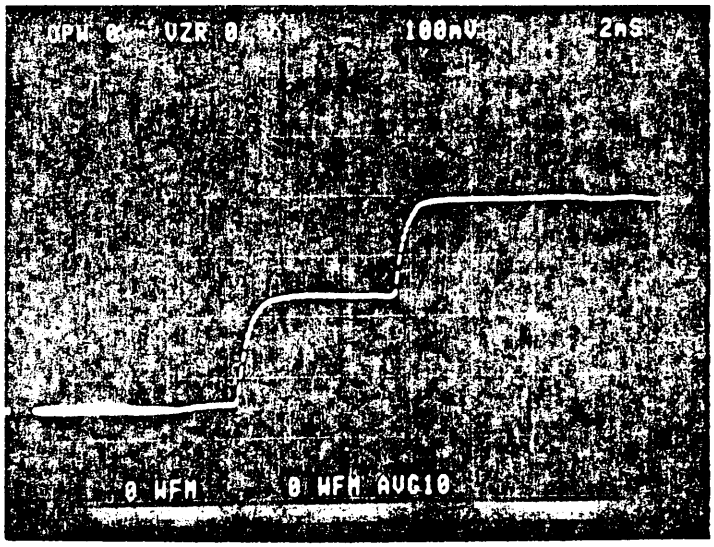

Figure 5.1.4.1 (a) FET strobe width too narrow (undersampling).

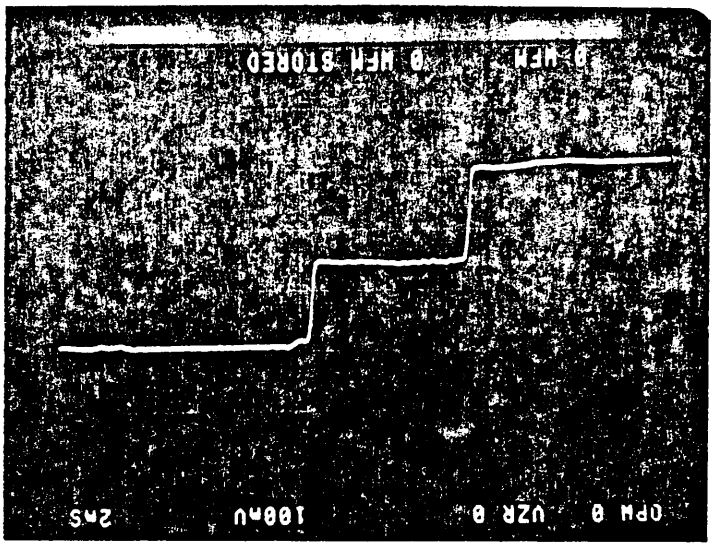

Figure 5.1.4.1 (b) FET strobe width correctly adjusted.

transmission line is varied from the open circuit to short circuit cases. The gain should be adjusted until there is no variation in the initial pulse amplitude in either termination. It may then be necessary to repeat the adjustments of the feedback and second sampler width slightly as these are dependant on amplifier gain. A requirement for later data analysis was to limit the gain of the output circuit to 300 mV for the open circuit case. This can be properly adjusted by changing P2 of the output circuit once all the other adjustments have been made.

5.2 Comparison of performance with commercial TDR units

The main emphasis of the design of a hybrid TDR was to reduce the size of the TDR to fit the soil moisture meter application and to increase the amplitude of the pulse. This last requirement was made to allow measuring moisture content in highly lossy soils. This was the reason for using a step recovery diode. The speed of the pulse was of less concern as the probe used is limited in bandwidth to about 1.5 GHz by the balun transformer. Even if the transition speed were increased, the balun would have been the limiting factor in any measurements.

Since the TDR is dedicated to the soil moisture meter application, increased pulse speed, variable fast ramp or other options were not necessary. The closest commercial TDR is the Tektronix 1502B and this unit was often used to compare the waveform generated by the hybrid TDR. The main comparison was of the cleanliness of the waveform. Since later data processing of the reflected waveform is to be accomplished by computer, a very clean waveform was necessary.

The Tektronix 1502B uses a tunnel diode pulse generator which limits the amplitude to approximately 0.5 volts (open circuit) with a transition duration $\lesssim$ 200 psec [22]. The ringing observed on the top of the waveform is about 10% of full scale. The hybrid TDR has an amplitude of 1.2 volts (open circuit) with a similar transition duration. The ringing was also slightly reduced to $\lesssim$8%. The result being well within the specifications desired.

Chapter 6

Summary and Conclusions

6.0 Summary

The objective of the thesis was to design a dedicated hybrid thick-film time domain reflectometer. It was intended that the process be flexible to allow for variation of the design according to the possible applications of this device.

Chapter 1 was an introduction to the thesis and briefly described the contents of each chapter.

Chapter 2 presented the concept of time domain reflectometry and the uses of this microwave measurement technique. Details of the measurement process required to obtain the moisture content of a soil sample using TDR were addressed. The frequency domain analogy to time domain measurements was also presented and a comparison of the hardware required for each technique was discussed.

Chapter 3 detailed the requirements for the electronics to produce the TDR unit. Particular attention was focused on the variety of pulse generator circuits and devices applicable to TDR systems. An equivalent time sampling scheme was presented along with the basic electronics required for its implementation. The overall timing and control functions were detailed along with their hardware versions. Adaptations and modifications to these subsystems as development of the TDR unit proceeded were discussed

Chapter 4 examined the technology of thick-film hybrid microelectronics and the process required for fabrication circuits using this technology. Special attention was given to the problems and advantages associated with microwave circuit manufacture using thick-film hybrids. A process was developed for transferring the electrical circuit diagrams to a functional hybrid layout. This design approach is applicable to any hybrid design.

Chapter 5 detailed the required steps necessary in testing the hybrid form of the electronics. A systematic approach for adjusting the unit for proper operation was also described and proper adjustments were documented.

6.1 Conclusions

The technique of time domain reflectometry can be used to characterize the electrical behavior of materials. This information can then be related to physical properties of the material itself. The application of moisture detection through delay measurement is easily accomplished using TDR. Problems can develop from the probe used to perform this measurement. Future effort in this application

should include designing a probe which does not distort the TDR waveform.

The fabrication of a dedicated thick-film hybrid time domain reflectometer was achieved. The design and design process is flexible to allow for application beyond the soil moisture meter. Controlling the TDR unit performance required multiple iterations in the physical layout of the circuit and component selection. Further work should investigate improving performance along a number of lines: Changes in material selection, substrate and conductor, may yield improved heat dissipation and reduced conductor loss. The timing signals may be modified to allow for variable sampling windows. The pulse generator section may be modified in characteristic impedance and pulse shape for use in new applications.

References

1. E. A. Wolff and R. Kaul, Microwave Engineering and Systems Applications, John Wiley and Sons, inc, New York, 1988.

2. J. W. Nilsson, Electric Circuits, Addison-Wesley Publishing Company, Massachusetts, 1983.

3. S. M. Riad and A. Elshabini-Riad, "RF and Wideband Hybrid Microelectronics", EE 5980 Lecture Notes, Virginia Polytechnic Institute, Blacksburg, 1987.

4. B. Ulriksson, "A Time Domain Reflectometer Using a Semiautomatic Network Analyzer and the Fast Fourier Transform", IEEE Transactions on Microwave Theory and Techniques, Volume MTT-29, Number 2, February 1981.

5. E. O. Brigham, The Fast Fourier Transform, Prentice-Hall, Englewood Cliffs NJ, 1974.

6. S. Y. Liao, Microwave Devices and Circuits, 2nd Edition, Prentice-Hall, ENglewood Cliffs NJ, 1985.

7. S. M. Riad, W. A. Davis, A. A. Riad, F. W. Stephenson, M. Ahmad, H. Geramifar, and A. M. Shaarawi, Electromagnetic Level Indicator: Design and Fabrication of the Time Domain Reflectometer, Final Report, David Taylor Naval Ship Research and Development Center, Virginia Polytechnic Institute, Blacksburg, 1983.

8. S. M. Sze, Physics of Semiconductor Devices, 2nd Edition, John Wiley and Sons, New York, 1981.

9. E. O. Kane, "Theory of Tunneling", Journal of Applied Physics, Volume 32, 1961.

10. S. M. Riad, M. Ahmad, A. A. Riad, and F. W. Stephenson, "The Design and Fabrication of Hybrid Thick FIlm Subnanosecond Pulse Generators", International Journal for Hybrid Microelectronics, Volume 5, Number 2, Reno NV, 1982.

11. Hewlett Packard, "Pulse and Waveform Generation with Step Recovery Diodes", HP Application note 918.

12. J. Andrews, Picosecond Pulse Labs, private communication.

13. J. Millman, Microelectronics, McGraw-Hill Book Company, New York, 1979.

14. Hewlett Packard, "Sampling Time Base and Vertical Amplifier", Operating and Service Manual, Hewlett Packard Company, Colorado, 1972.

15. J. Mulvey, Sampling Oscilloscope Circuits, Tektronix Inc., Beaverton Oregon, 1970.

16. A. Elshabini-Riad, "Hybrid Microelectronics", EE4200 Lecture Notes, Virginia Polytechnic Institute, Blacksburg VA, 1987.

17. A. B. Glaser and G. E. Subak-Sharpe, Integrated Circuit Engineering, Addison-Wesley Publishing Company, Massachusetts, 1979.

18. C. A. Harper, Ed., Handbook of Thick Film Microelectronics, McGraw-Hill Book Company, New York, 1974.

19. E. I. DuPont, Thick Film Conductor Data Sheets, 1988.

20. E. I. DuPont, Thick Film Dielectric Data Sheets, 1988.

21. A. A. Riad, S. M. Riad, M. Ahmad, F. W. Stephenson, and R. A. Ecker, "Thick-Film Coplanar Strip and Slot Transmission Lines for Mcrowave and Wideband Integrated Circuits", International Journal for Hybrid Microelectronics, Volume 5, Number 2, Reno NV, 1982.

22. T. Pekala, Tektronix Inc., private communication.

23. J. R. Andrews, B. A. Bell, and E. E. Baldwin, "Reference Flat Pulse Generator", NBS Technical Note 1067, U. S. Government Printing Office, Washington DC, 1983.

The vita has been removed from the scanned document